

Summer 7-2016

Surface Roughness Effects on Light Propagation in Optical Light Pipes

Youngjin Park

Rose-Hulman Institute of Technology, parky2@rose-hulman.edu

Follow this and additional works at: http://scholar.rose-hulman.edu/optics_grad_theses



Part of the [Engineering Commons](#), and the [Optics Commons](#)

Recommended Citation

Park, Youngjin, "Surface Roughness Effects on Light Propagation in Optical Light Pipes" (2016). *Graduate Theses - Physics and Optical Engineering*. Paper 14.

This Thesis is brought to you for free and open access by the Graduate Theses at Rose-Hulman Scholar. It has been accepted for inclusion in Graduate Theses - Physics and Optical Engineering by an authorized administrator of Rose-Hulman Scholar. For more information, please contact weir1@rose-hulman.edu.

Surface Roughness Effects
on Light Propagation in Optical Light Pipes

A Thesis

Submitted to the Faculty

of

Rose-Hulman Institute of Technology

by

Youngjin Park

In Partial Fulfillment of the Requirements for the Degree

of

Master of Science in Optical Engineering

July 2016

© 2016 Youngjin Park



ROSE-HULMAN INSTITUTE OF TECHNOLOGY

Final Examination Report

Youngjin Park Optical Engineering
Name Graduate Major

Thesis Title Surface Roughness Effects on Light Propagation in Optical Light Pipes

DATE OF EXAM:

EXAMINATION COMMITTEE:

	Thesis Advisory Committee	Department
Thesis Advisor:	Robert Bunch	PHOE
	Sergio Granieri	PHOE
	Wonjong Joo	SNUST

PASSED FAILED

ABSTRACT

Park, Youngjin

M.S.O.E.

Rose-Hulman Institute of Technology

July 2016

Surface Roughness Effects on Light Propagation in Optical Light Pipes

Thesis Advisor: Dr. Robert M. Bunch

Solid- and hollow-core light pipes are commonly employed to shape the intensity profile of high power lasers for applications in various technology industries such as the automobile, medical, and communications. There are several loss mechanisms present in solid-core glass and polymer light pipes, including absorption, bulk scattering in the material, surface scattering at the material-air interface, and Fresnel Loss at the material-air interface. Fresnel reflection and surface scattering losses typically dominate over other loss mechanisms in solid-core light pipes made of high quality optical materials. In order to analyze the losses in the light pipe, an approximate model is developed and tested using glass and polymer light pipes. The experiments in this thesis focus on analysis of the scattering loss in several optical light pipes configurations. From this analysis, the surface roughness parameters can be determined based on models and comparing with other measurements.

ACKNOWLEDGEMENTS

I would like to express my gratitude to my supervisor, Robert M. Bunch, whose expertise, understanding, patience, and encouragement throughout my study and research while pursuing my master's degree. Without his incredible patience and timely wisdom and counsel, my thesis work would have been a frustrating and overwhelming pursuit. It was truly an honor for me. Your insight, enthusiasm, and dedication to me were very helpful in my studies. I have thoroughly enjoyed all of our discussions, both educational and technical, and am grateful that your door was always open. I could not have finished this study without you. I also thank Professor Sergio C. Granieri and Paul O. Leisher for supporting my thesis

I would also like to thank Professor Wonjong Joo, my advisor in Seoultech. He always helps me with my course work and inspires me that I can do everything.

I thank the Physics and Optical Engineering and the Graduate Departments at Rose-Hulman Institute of Technology, and Manufacturing Systems and Design Engineering Department at Seoultech for their support and the opportunities that they have given to me.

I would like to show appreciation to my friends; Guebum, Kang-min, Gregory, Grant, Deepak, John-Michel, and Austin. They were always willing to help and give their best suggestions.

Finally, I would like to thank my father, mother, and sister for their unconditional love and support during the last two years. I would not have been able to complete this thesis without their continuous love and encouragement.

TABLE OF CONENTS

LIST OF FIGURES	iv
LIST OF TABLES	vi
LIST OF ABBREVIATIONS	vii
LIST OF SYMBOLS	viii
1. Introduction	1
2. Theory	5
2.1 Absorption loss	5
2.2 Bulk Scattering in Material.....	7
2.3 Total Integrated Scattering (TIS).....	1 0
2.4 Fresnel Reflection loss at interface	1 1
3. Design Surface Roughness Analysis Model	1 5
3.1 Light loss analysis model background	1 5
3.2 Design analysis model in Microsoft Excel and Matlab	1 8
4. Experiments	2 4
4.1 Experimental set-up and procedure for measuring incident light and transmitted light	2 5
4.2 Experimental set-up and procedure for assuming mean free path	2 7
4.3 Other methods for measuring surface roughness	3 2
5. Results and Discussion	3 5
5.1 Results of the mean free path and reflection los coefficient.....	3 5
5.2 Calculate the surface roughness RMS value.....	3 8
5.3 The surface roughness measured by other measurements	4 5

5.4 Error analysis	4 6
6. Conclusions and Future work	4 9
LIST OF REFERENCES.....	5 1
APPENDIX A: Analysis model in Excel	5 4
APPENDIX B: Analysis model code in Matlab.....	6 0

LIST OF FIGURES

Figure	Page
Figure 1.1: Specimens	2
Figure 2.1: Simplified visualization: an incident EM wave scattered by a particle	7
Figure 2.2: Simplified visualization of a the light wave propagating through a material	8
Figure 2.3: The light beam scattering at the rough surface [14]	10
Figure 2.4: (a) Electric field is parallel to incident surface (TE mode, S-polarized), (b) Magnetic field is parallel to incident surface (TM mode, P-polarized)	13
Figure 3.1: Images of flex guide in PMMA light pipe from 0 degree to 50 degrees, 5 degree increments	15
Figure 3.2: The light loss mechanisms conceptual diagram	16
Figure 3.3: The relationship chart between each step of the process used in the analysis model and experimental comparison	21
Figure 4.1: Experimental set up for applying to analysis model	26
Figure 4.2: Experimental set up for determining mean free path	27
Figure 4.3: The graph of the experimental results to measure mean free path. The graphs indicate the log of the transmittance versus total length of the specimen. In the experimental results using single specimen and using two specimens, five and eight experimental results are used for calculate the mean free path.....	29
Figure 4.4: Schematic diagram illustrating the geometrical analysis used for same length specimens	30

Figure 4.5: The top view of the experiment for measuring the mean free path using single and multiple PMMA light pipes	3 2
Figure 4.6: Surface roughness measurements (a) New View Zygo Interferometer (New View 6300), (b) Atomic Force Microscope (easyScan DFM)	3 4
Figure 5.1: Experimental results to calculate the mean free path.....	3 6
Figure 5.2: Comparing the amount of the light propagation for 0 degree incident angles	3 7
Figure 5.3: the graphs of comparing the experimental results and the calculation results: well-polished acrylic light pipe (a) 5.5 inch, (b) 6 inch, (c) 6.5 inch, and (d) 7 inch	4 0
Figure 5.4: Comparison between the experimental results and the calculation results: (a) PMMA light pipe (5 inch) and (b) Glass light pipe (10cm)	4 0
Figure 5.5: Comparison of the experimental results and the calculation results: Acrylic light pipe fabricated by laser (a) 5.5 inch, (b) 6 inch, (c) 6.5 inch, and (d) 7 inch and (e) Curved acrylic light pipe fabricated by laser.....	4 1
Figure 5.6: Comparison of the experimental results and the calculation results: (a) PMMA light pipe (5 inch) and (b) Glass light pipe (10cm)	4 2
Figure 5.7: Comparing the calculation results and range of surface roughness RMS when using well-polished specimen.....	4 8
Figure 5.8: (a) the surface profile of Al light pipe fabricated by milling, (b) Shape of the transmitted light pattern at 10 degrees in the well-polished Al light pipe, and (c) similar pattern for the Al light pipe fabricated by milling.	4 8

LIST OF TABLES

Table	Page
Table 3.1: Parts of the analysis model; (a) Basic input part, (b) experimental results part	1 9
Table 5.1: The results of the mean free path and reflection loss coefficient	3 7
Table 5.2: A summary of all the results of surface roughness calculated by the analysis model.....	4 4
Table 5.3: Experimental results of surface roughness measured by AFM and New View Zygo interferometer	4 5
Table 5.4: Summary of the results of surface roughness RMS including experimental error and differences between the model calculations and experimental values..	4 6
Table A.1: Calculation steps of the analysis model (Step (1): bulk scattering length, Step (2): Bulk scattering loss at each point, Step (3): light power before roughness scattering point, Step (4): roughness scattering loss at each point, and Step (5) Light power after roughness scattering)	5 6
Table A.2: Calculating transmitted light power with each loss coefficients	5 7
Table A.3: Verify energy conservation in the analysis model	5 8
Table A.4: Surface roughness calculation using ‘Solver’ function in Microsoft Excel	5 9

LIST OF ABBREVIATIONS

AFM	Atomic Force Microscope
MFP	Mean Free Path
PMMA	Poly (methyl methacrylate)
RMS	Root Mean Square
TE	Transverse Electric
TIS	Total Integrated Scattering
TM	Transverse Magnetic

LIST OF SYMBOLS

Mathematical Symbols

C The concentration of molecule

R_q Root means square roughness

R_a Roughness average

ϵ_0 Permittivity of free space

μ_0 Permeability of free space

μ The attenuation coefficient

σ Root mean square roughness

1. Introduction

Light loss in optical light pipes has been an important issue in various technology industries such as the automobile, medical, and communications. In particular, bulk scattering and surface roughness scattering make it more difficult to model and predict light distributions and illumination levels. Analyzing light loss is a useful indicator for the study of specimen qualities in various conditions such as purity of specimen and surface roughness. Because of this, the methods of analyzing the light loss have been researched.

The purpose of this study was to develop and test an analysis model for the light loss in optical light pipes that allows for light loss to be calculated at any point in the specimen and to analyze the effect of the scattering loss due to surface roughness. In order to verify reliability of the analysis model, we used various light pipe specimens which have different optical and physical characteristics such as specimen length, medium, surface roughness, etc. Also, the analysis model is verified by comparing with other surface roughness measurements.

As shown in Fig. 1.1, several different types of the specimens were used for comparison. Several lengths of solid acrylic light pipes (5inch, 5.5inch, 6inch, 6.5inch, and 7inch), a PMMA light pipe, and a glass light pipe were used. In the case of the acrylic light pipe, the surfaces in opposition to each other were either well-polished surfaces or laser cut surfaces. The PMMA light pipe was specially fabricated with particles embedded into the bulk of the material to generate more scattering. Also, the PMMA light pipe and the glass light pipe were well polished. Generally, the light pipes have many different shapes as well as rectangular parallelepiped in the industry. A curved acrylic light pipe was also fabricated for these tests. In addition, a hollow core

light pipe was made to verify the analysis model since the only contribution to the light loss is surface scattering. Two types of hollow core light pipes were made, one using mirrors and the other a machined Al light pipe. We polished the mirrors by hand using LINDE A 0.3 microns Alumina powder in order to introduce a known scattering loss with a predictable surface roughness RMS. Also, two different surface conditions of the machined Al light pipes were used.

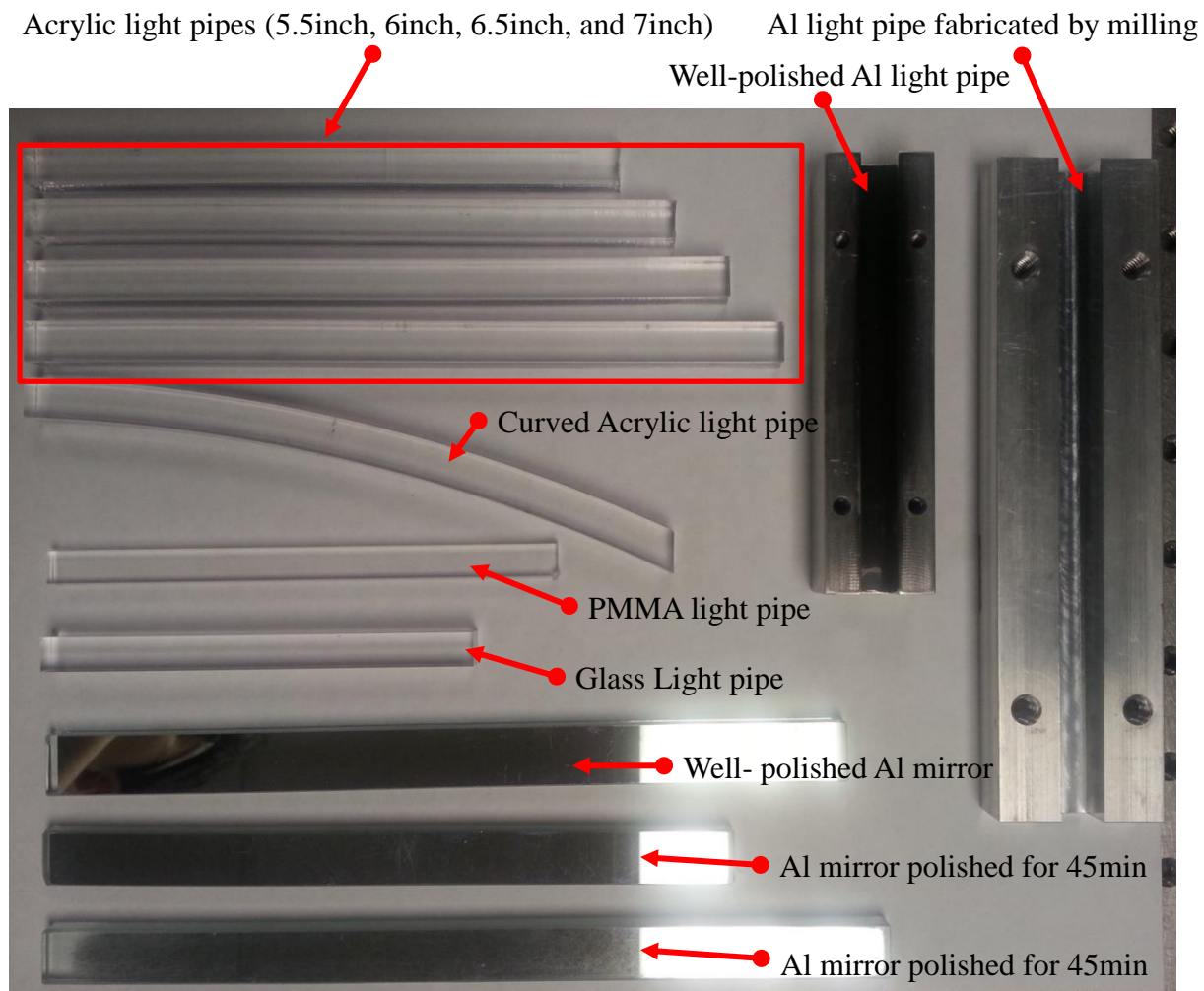


Figure 1.1: Specimens

In Chapter 2, the light loss in the light pipe will be discussed theoretically. There are several loss mechanisms which are absorption, bulk scattering in the material, scattering from rough surface at the material-air interface, and Fresnel reflection loss at the material-air interface. These losses can be explained by the Beer-Lambert law, total integrating scattering, and Fresnel equations.

Chapter 3 describes the analysis model for analyzing light loss and calculating the surface roughness. Through the previously mentioned light loss theories, the analysis model is computed using Excel and Matlab programs. The analysis model consists of five parts which are: physical parameter input variables, calculation light loss at each point, calculation of total loss, verification, and calculation of surface roughness. This chapter focuses on an explanation of the mechanisms used in the analysis model and how these values are calculated in Excel. Details of the Excel computations are given in Appendix A. The Matlab code is attached at Appendix B.

The experimental verification of the model is described in Chapter 4. Depending on the type of specimen, two different experiments were performed. For the solid light pipes, a procedure to measure the mean free path related with absorption loss and bulk scattering loss was used. The second experiment was a direct measurement of the transmitted light power. Also, the surface roughness of each specimen was measured by "New View Zygo interferometer 6300" and atomic force microscopy (AFM) in order to verify the surface roughness calculated by the analysis model.

Finally in Chapter 5, the experimental results and analysis results are discussed. The solid specimens have a mean free path from $509.4\mu\text{m}$ to $8859.3\mu\text{m}$. As expected, the transmitted light

power experiments showed that the more scattering particles or rougher surface at the side of the specimen, the less the transmitted light is detected at the end of the light pipes. Comparing the surface roughness values from the analysis model and other measurements, the loss rate is around 10% higher for the analysis results than the measurement results of a well-polished specimen.

2. Theory

In this chapter, the types of light power loss in the light pipe are briefly introduced and these theories are used to develop a model that describes the light propagation through the light pipe and losses within the light pipe. The model includes characteristics such as surface roughness, mean free path, and material properties of the guide. This thesis focuses on light power loss at each point and surface roughness.

In an optical light pipe, light loss can be classified into four different groups. There are surface scattering due to the roughness at various surfaces, bulk scattering by small particles and density fluctuations within the material, Fresnel reflection loss, and absorption loss in the material.

2.1 Absorption loss

When a source of light penetrates a clear material, various phenomena occur at the microscopic level. In the material, diverse atoms and molecules contain electrons. Their attached springs and these electrons tend to vibrate at specific frequencies. Similar to a musical instrument and radio performance property, the electrons in atoms are vibrated at a natural frequency. The electrons in the atom are set into vibrational motion when a light wave and an atom which have same natural frequency are bumped against each other. Those electrons which are impacted with a light wave will absorb the energy of the light wave and transform it into vibrational motion. Vibrating electrons have an influence on nearby atoms in such manner as to

transform their vibrational energy into thermal energy [1][2]. In this process, some light waves penetrate the material and others are absorbed by the material and the energy released through other mechanisms such as thermal energy [3].

The Beer-Lambert law is commonly used to analyze light wave absorption in a material [4]. This is combined with Lambert's law and Beer's law. When a ray of light passes through absorbing medium, Lambert's law indicates that light intensity decreases exponentially as the propagation distance in a medium increases and Beer's law shows that the intensity decreases exponentially as the concentration of molecule in medium increases [4]. These laws are valid in Gamma rays and radio wave as well as in visible rays. It will be explained detail in next chapter because it includes absorption loss and bulk scattering loss.

Lambert law is written as,

$$I = I_0 e^{-k_1 l} \quad (2.1)$$

and Beer's Law as,

$$I = I_0 e^{-k_2 C} \quad (2.2)$$

Where k_1 and k_2 are each different extinction coefficient, C is the concentration of molecule, and

l is propagation distance in material

2.2 Bulk Scattering in Material

Bulk scattering can be defined as the redirection of radiation out of the original direction of electromagnetic wave propagation because of interactions with molecules and small particles and occurs only in the bulk of the optical material. When an EM wave makes contact with a small particle, the electron orbits are influenced by the particle's molecules which vibrate with the same frequency as the electric field of the incident wave as shown in Fig. 2.1. The oscillating electron clouds results in a periodic separation of charge within the molecule. This oscillating induced dipole moment becomes an effective source of electromagnetic radiation with an identical frequency to the incident light [5-7]. In this situation we call the type of scattering, elastic scattering since the scattered light is the same frequency as the incident light.

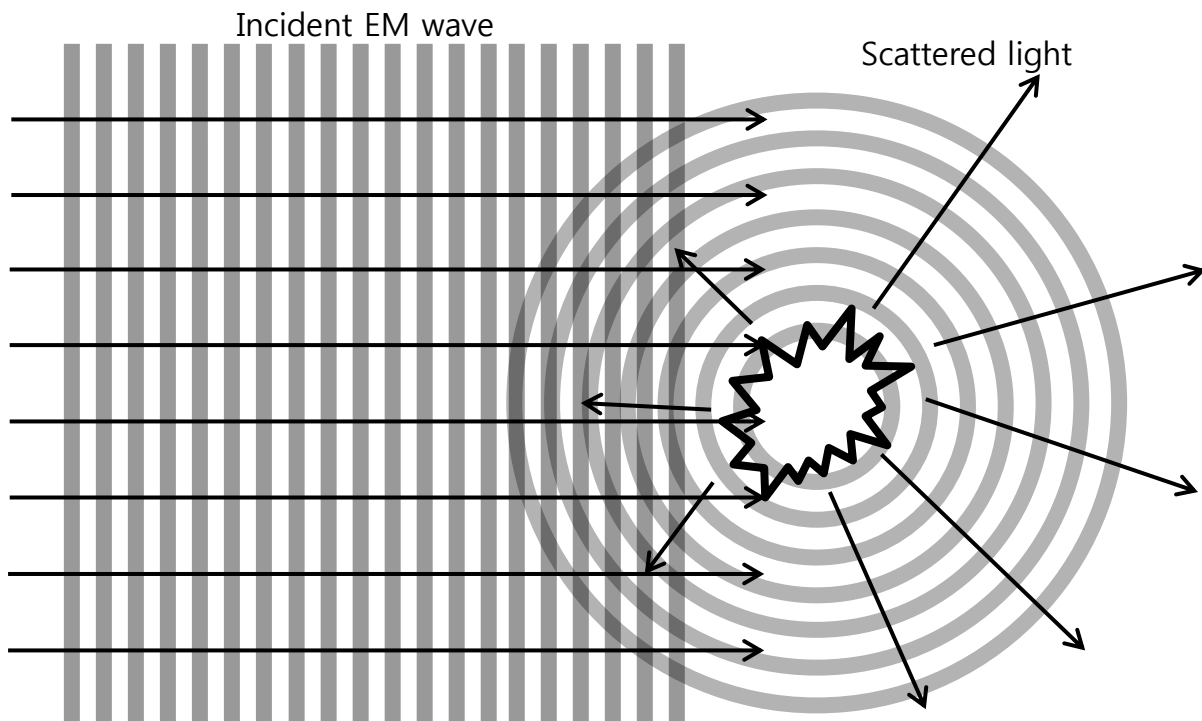


Figure 2.1: Simplified visualization: an incident EM wave scattered by a particle

Generally, there are two main types of elastic light scattering theory, Rayleigh scattering and Mie scattering. Rayleigh scattering indicates that scattering occurs when the size of particles that induce the scattering is smaller than the wavelength of light. The scattered intensity for Rayleigh scattering is inversely proportional to the fourth power of the wavelength [8]. This means that the scattered intensity for high wavelengths will be reduced drastically from the amount of light scattering for short wavelengths. Mie scattering occurs when the particle size is similar to the wavelength of the light and the scattering is more influenced by the molecular density than the wavelength. Examples of this scattering are water vapor, ice particles and smoke. Rayleigh scattering and Mie scattering are used for describing most spherical particle scattering systems.

The scattering loss by small particles is expressed by the Beer-Lambert law which explains the Absorption loss by the medium as well as the bulk scattering loss. We illustrate the Beer-Lambert law with simple examples. Figure 2.2 shows that incident light ($I_\lambda(0)$) enters the material and transmitted light ($I_\lambda(s_1)$) comes out from the material.

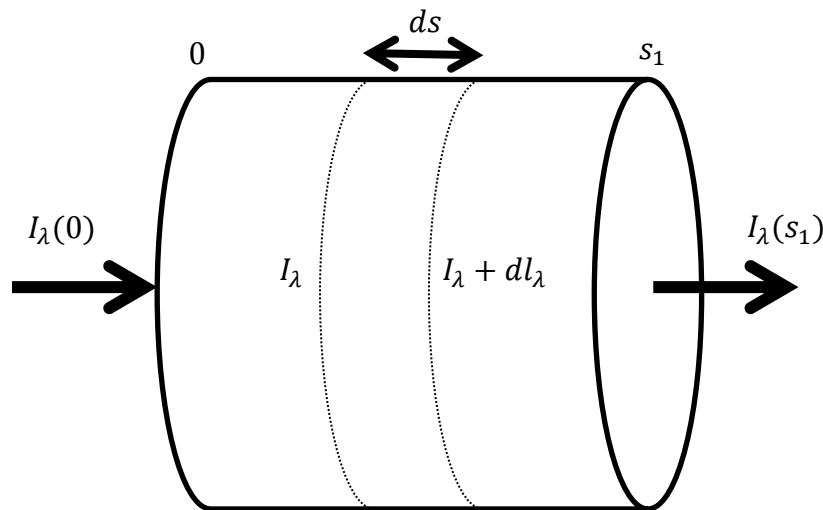


Figure 2.2: Simplified visualization of a the light wave propagating through a material

If the incident light area is 'A' and material thickness is 'dx' and concentration of molecules is 'C', the number of molecules which are illuminated by the incident light (I_λ) is $CA dx$. The total effective area of the molecules is $\sigma CA dx$; σ is effective absorption cross-section per molecule. The probability of light which is absorbed and scattered in the material is as follows,

$$-\frac{dI_\lambda(x)}{I_\lambda(x)} = \frac{\sigma CA}{A} dx \quad (2.3)$$

When light is traveling in the specimen, both bulk scattering and absorption occur constantly. By integrating both sides of Eq. (2.3), total of the bulk scattering loss and the absorption loss can be calculated. Also, we can compute the relationship between incident light and transmitted light.

$$\int_{I_\lambda(0)}^{I_\lambda(s_1)} \frac{dI_x}{I_x} = - \int_0^{s_1} \sigma C dx \quad (2.4)$$

Where S_1 is the propagation length in the specimen

The interval of integration is from 0 to S_1 . We can find the relationship between the incident light power and the transmitted light power by solving Eq. (2.4).

$$\ln(I_\lambda(s_1)) - \ln(I_\lambda(0)) = \ln\left(\frac{I_\lambda(s_1)}{I_\lambda(0)}\right) = -\sigma C S_1 \quad (2.5)$$

$$I_\lambda(s_1) = I_\lambda(0) e^{-\sigma C S_1} \Rightarrow I = I_0 e^{-\sigma C x} = I_0 e^{-\mu x} \quad (2.6)$$

Where μ is the attenuation coefficient defined as σC

The result of Eq. (2.6) shows that the light intensity decreases exponentially with length in the material. The attenuation coefficient includes absorption coefficient and scattering

coefficient and is also inversely related to mean free path (MFP). The MFP indicates that the average distance a photon travels between collisions with atoms in the specimen [9]. It depends on purity of the material and kind of material.

2.3 Total Integrated Scattering (TIS)

As shown in Fig. 2.3, when a beam of a laser is directed towards a rough surface, the reflected light field consists of a specular reflection beam and scattered light. Total integrated scattering (TIS) has been developed to determine the surface roughness RMS value from the ratio between intensity of the incident light and the scattered light [10]. In order to analyze this scattered light, Bennett and Porteus suggested the concept of TIS and the theoretical relationship between TIS and the root mean square surface roughness parameter [11][12]. This theory is influenced from the paper “the reflection of electromagnetic radiation from a rough surface” which derived by Davies [13]. Although this paper was related with the scattering of radar waves from rough water surfaces, it can be also applied to light waves.

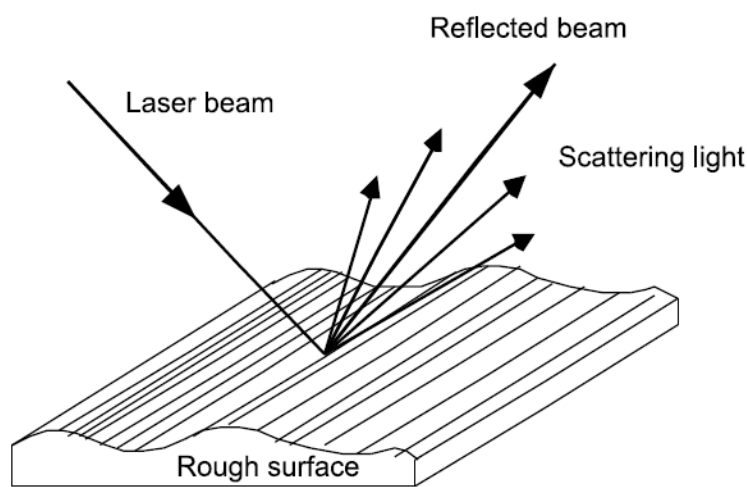


Figure 2.3: The light beam scattering at the rough surface [14]

The TIS model must follow two conditions: (1) the root mean square roughness parameter is small compared with the wavelength, and (2) The surface condition is smooth and well-polished [15][16]. The TIS model which indicates the relationship between surface scattering and surface roughness is as follows,

$$\text{TIS} = R_0 \left[1 - \exp \left[- \left(\frac{4\pi\sigma \cos \theta_i}{\lambda} \right)^2 \right] \right] \quad (2.7)$$

Where R_0 is the reflectance of the surface, σ is the root mean square roughness which is sometimes represented as R_q , θ_i is the incident angle, λ is the wavelength of the laser source.

Several conclusions can be drawn from equation (2.7) regarding TIS. First, the scattering is only related to the root mean square surface roughness. Second, surface reflectance is proportional to the amount of scattered light. Third, the shorter the wavelength, the bigger the amount of scattering by the surface roughness. And finally, light at normal incidence produces more scattering than grazing incidence light.

The parameters R_q and Mean roughness (roughness average, R_a) are both useful expressions for characterizing surface roughness, but they are calculated differently. R_q is calculated as the root mean square of the surfaces roughness. R_a is calculated as a roughness average of the surface roughness. In general, R_q values are 1.1~1.4 times the R_a values because R_q has larger deviation than R_a [17][18].

2.4 Fresnel Reflection loss at interface

When light moves from one medium to another medium, some light is reflected at the boundary surface and the remainder is transmitted through the medium. According to electromagnetic theory, when a plane electromagnetic wave arrives at the boundary surface

between two different types of mediums, it will separate as a transmitted wave and a reflected wave. The transmitted wave and the reflected wave are influenced by polarization of the incident wave, incident angle, and refractive index [19][20]. A summary of this is described through the Fresnel equations.

The Fresnel equations describe how much of the light is reflected and how much of the light is transmitted. Also, the amount of transmission and reflection are influenced by the polarization direction of the incident light. When a light were encounters the boundary between two media, Maxwell's equation and boundary conditions must be satisfied [21][22].

Maxwell's equation

$$\nabla \cdot \mathbf{E} = \frac{\rho}{\epsilon_0} \text{ (Gauss's law)} \quad (2.8)$$

$$\nabla \cdot \mathbf{B} = 0 \text{ (Guass's law for magnetism)} \quad (2.9)$$

$$\nabla \times \mathbf{E} = -\frac{\partial \mathbf{B}}{\partial t} \text{ (Faraday's law)} \quad (2.10)$$

$$\nabla \times \mathbf{B} = \mu_0 \mathbf{J} + \mu_0 \epsilon_0 \frac{\partial \mathbf{E}}{\partial t} \text{ (Ampere's law)} \quad (2.11)$$

There are two different cases depending on the polarization of the incident light. One is s-polarized which the incident light is polarized with the electric field perpendicular to the plane. Another is p-polarized which the incident light is polarized with the electric field parallel to the plane.

Figure 2.4 shows two different modes; (a) transverse electric modes (TE mode) and (b) transverse magnetic modes (TM mode). In case of the TE mode, the electric field \mathbf{E} is perpendicular to interface and in the same plane as the magnetic field \mathbf{B} . On the contrary, when the magnetic field \mathbf{B} is perpendicular to the interface and in the same plane as the electric field \mathbf{E} ,

this is the TM mode. The propagation vectors of both E and B should satisfy Fleming's right hand rule.

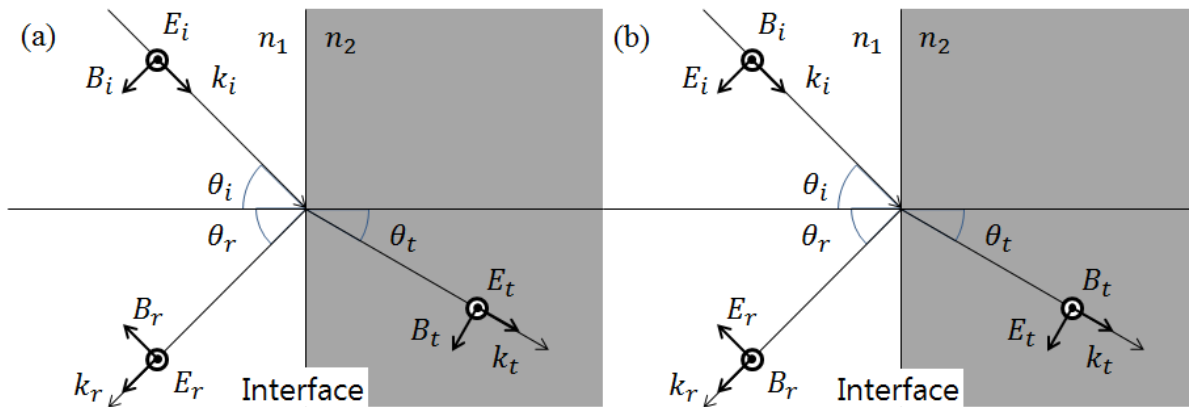


Figure 2.4: (a) Electric field is parallel to incident surface (TE mode, S-polarized), (b) Magnetic field is parallel to incident surface (TM mode, P-polarized)

In order to obtain the Fresnel equations, we need two more boundary conditions as well as Eq. (2.12). If the boundary plane is an infinite plane between two medium and there are no free electron at boundary, the boundary condition is that normal vector of E and B are continuous and tangential vector of them are continuous. The first boundary condition is that tangential lines of the electric field E and magnetic field B have to come into existence about the boundary conditions at any points. Another boundary condition is that tangential components of magnetic field B at TE mode and electric field E at TM mode are constant. The boundary conditions are as follows,

$$\mathbf{k} \times \mathbf{E} = \nu \mathbf{B} \quad (2.12)$$

$$\mathbf{k} \cdot \mathbf{E} = 0$$

$$E_{oi} + E_{or} = E_{ot} \quad (2.13)$$

$$TE \text{ mode} : -\frac{B_i}{\mu_i} \cos \theta_i + \frac{B_r}{\mu_r} \cos \theta_r = -\frac{B_t}{\mu_t} \cos \theta_t \quad (2.14)$$

$$TM \text{ mode} : \frac{1}{\mu_t \nu_t} E_i + \frac{1}{\mu_t \nu_t} E_r = -\frac{1}{\mu_t \nu_t} E_t$$

Where μ_i , μ_r , and μ_t is the respective permeability of the incident medium reflected medium and transmitted medium.

Using wave Eq. (2.13) and (2.14), if Permeability coefficient is not changed, the amplitude reflection coefficient (R) and amplitude transmission coefficient (T) are as follows,

TE mode (S-polarized)

$$R = \left| \frac{n_i \cos \theta_i - n_t \cos \theta_t}{n_i \cos \theta_i + n_t \cos \theta_t} \right|^2, T = \left| \frac{2n_i \cos \theta_i}{n_i \cos \theta_i + n_t \cos \theta_t} \right|^2 \quad (2.15)$$

TM mode (P-polarized)

$$R = \left| \frac{n_t \cos \theta_i - n_i \cos \theta_t}{n_i \cos \theta_t + n_t \cos \theta_i} \right|^2, T = \left| \frac{2n_i \cos \theta_i}{n_i \cos \theta_t + n_t \cos \theta_i} \right|^2 \quad (2.16)$$

In this case, n_i is the refractive index of the incident medium and n_t is the refractive index of the transmitted medium.

3. Design Surface Roughness Analysis Model

3.1 Light loss analysis model background

In the previous chapter, the light loss theories used in the analysis model were discussed. In this chapter, the light loss analysis model is introduced based on these scattering theories. Figure 3.1 shows a laser beam propagating within a PMMA optical light pipe with incident angle of 0 degree to 50 degrees, 5 degree increments with respect to the normal to the incident surface.

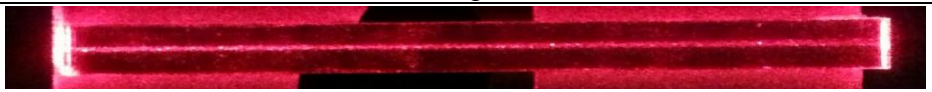
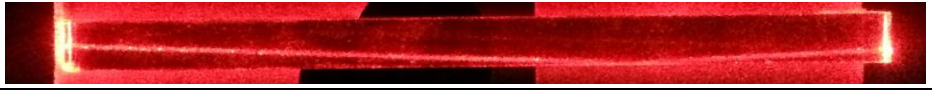
Rotation Angle	Images
0°	
5°	
10°	
15°	
20°	
25°	
30°	
35°	
40°	
45°	
50°	

Figure 3.1: Images of flex guide in PMMA light pipe from 0 degree to 50 degrees, 5 degree increments

The laser beam paths are visible because of scattering from particles within the medium. If the material is very pure, the laser paths are difficult to see such as in an air medium. The large amount of scattered light at the incidence surface, back surface, and total internal reflection points at the boundary surface is caused by surface roughness scattering. Also, the more the incident angle is increased, the more the amount of scattering is increased. The light loss analysis model in optical light pipe is designed based on this phenomenon.

When a light beam is incident on a transparent material slab, the light will propagate as shown in Fig. 3.2 (a). To model this propagation, the Fresnel reflection loss, bulk scattering loss, surface roughness scattering loss, and absorption must be included. Figure 3.2 (b) shows the light ray incident at an angle of 20 degrees.

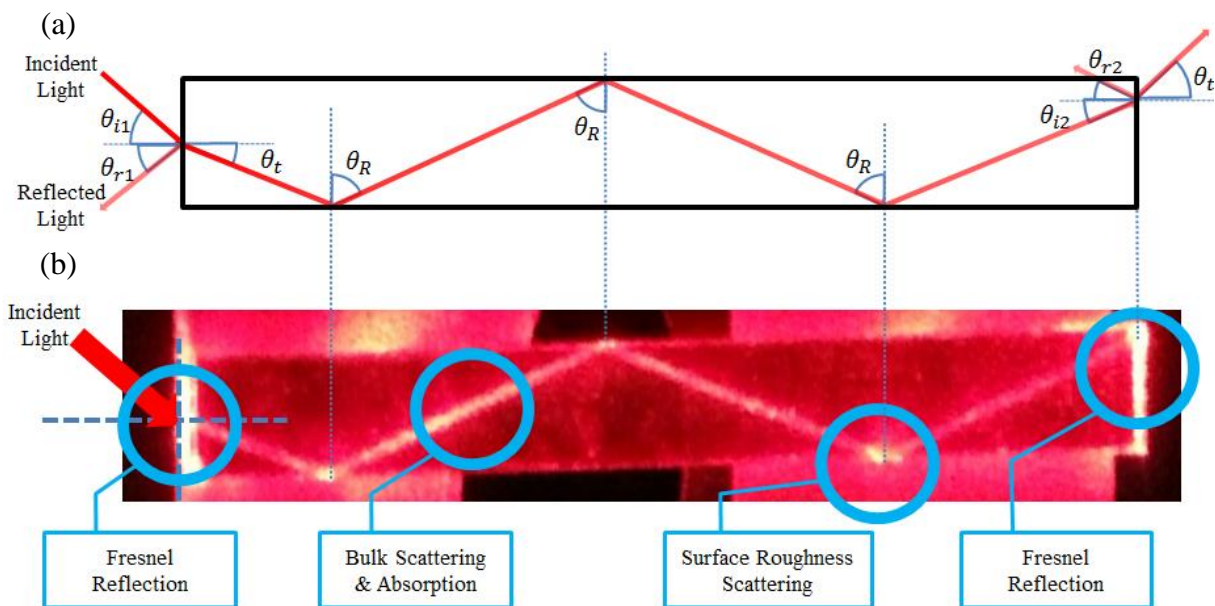


Figure 3.2: The light loss mechanisms conceptual diagram

As the light propagates from the air into the material on the left surface, both reflection and refraction of the light occurs which is described by Fresnel reflection theory [20]. Some light is refracted in the material and the remainder is reflected in air. In practice, because the incident surface is not completely smooth, the transmitted light power is further decreased by surface roughness scattering. As the transmitted beam propagates, the refracted light continues to lose energy because of material absorption and bulk scattering by very small particles in the material. The light which already has experienced optical losses is also influenced by the surface roughness scattering at the total internal reflection from the side surface of the material. The amount of surface scattering can be expressed by the TIS model suggested by Bennett and Porteus [11]. Total internal reflection is able to occur there because the side surfaces are located between different refractive index areas. However, in this research, we used the specimens which have refractive index around 1.48 and total internal reflection occurs at the side surface because the incident angle is higher than the critical angle (around 42.1 degree). Therefore, there are three major contributions to the loss of light on a beam propagating in a symmetric light pipe, Fresnel reflection, surface roughness scattering, and bulk scattering & absorption. These losses are expressed in Eq. (2.6), (2.7), and (2.15). So, transmitted light power can be calculated as follows,

$$\begin{aligned} \text{Transmitted light Power} = & (1 - \text{First Fresnel Reflection Loss ratio}) \\ & \times (1 - \text{Roughness Scattering Loss ratio})^n \\ & \times (1 - \text{Bulk Scattering Loss ratio}) \\ & \times (1 - \text{Second Fresnel Reflection Loss ratio}) \end{aligned} \quad (3.1)$$

Where n is the number of the reflections in the optical light pipe.

In Eq. (3.1), variable values are wavelength of light, mean free path in the material, refractive index of the material, incident angle, propagation distance, and roughness RMS value. Material properties such as mean free path and refractive index and wavelength of light source

are constant values. Also, the propagation distance is able to be calculated easily because it is changed depending on incident angle. Through inverse calculation based on these values, the roughness RMS value can be determined. In order to analyze the amount of light loss and the roughness RMS, we used analysis programs written in both Microsoft Excel and Matlab.

3.2 Design analysis model in Microsoft Excel and Matlab

Based on scattering loss theories, a surface roughness analysis model for light propagating in optical light pipes was developed for calculations in Microsoft Excel and Matlab. For the Excel calculations, the analysis model is separated into several parts in order to calculate the light loss systematically. This process will be explained using the PMMA light pipe as an example.

The first part of the process involves entering known physical variables as input information. Table 3.1 (a) shows how the basic information of material, wavelength and refractive index is input to the model. In the process of filling out part (a), it is important to note that some value of the surface roughness must be entered (such as 0.1 micrometer) as a starting point. If the surface roughness value is blank (the assumed value of zero), the analysis model will not provide a proper change. Also, the mean free path is an unknown value. But this quantity will be determined from experimental results. The application of this model to experiments will be introduced in Chapter 4. Table 3.1 (b) shows the worksheet section used to input measurement data. The input light power must be provided from the measurement for calibration. The output

column to the right is used to provide a normalized data set for any desired input (shown in the table as 1.0).

Table 3.1: Parts of the analysis model; (a) Basic input part, (b) experimental results part

(a) Specimen Information	Width	8mm
	Height	4mm
	Length	121mm
	Roughness (RMS)	0.1 μ m
	Reflective Index	1.4815
	Mean Free Path	509.4 μ m
	Experiment Condition	
	Reflective Index	1
	Wavelength	0.632 μ m

(b) Input power	1.241	→	1.000
Incident angle	Output		
0°	0.902	→	0.727
5°	0.890		0.717
10°	0.878		0.707
15°	0.844		0.680
20°	0.802		0.646
25°	0.762		0.614
30°			
35°			
40°			

After all input variables and measured data are entered then the initial calculations can be accomplished using the equations about light loss. The detailed step by step process described below. Once these calculations are completed then the transmitted light power is calculated and checked against the experimental data. The ‘solver’ function in Excel is used to adjust the surface roughness value to find a best fit to the data.

The result of these calculations is designed in order to model the light loss at any point in the specimen. There are five different steps involved in the calculation procedure. Figure 3.3 shows a flow chart diagram of the relations between each step in the calculation. We calculate the amount of light loss in the order in which the loss occurs within the specimen, once the beam has attained energy losses by bulk scattering and absorption. These losses are related with

propagation length in the specimen. The loss due to multiple propagation lengths are summarized in detail in Table A.1 (a). In step 2, the bulk scattering losses with absorption loss at each point are calculated using Eq. (2.6) based on the step1 data and step5 data. In order to analyze light loss by surface roughness at each point, we need the light power before the first reflection has happened at the side surface of specimen. This process is step 3 and summarized in detail in Table A.1 (c). In step 4, the roughness scattering loss at each point can be calculated by Eq. (2.7). Like step 3, in order to know the bulk scattering and the absorption loss at each point, we need the light power after the reflection occurs. That value is found in step 5 and influences the quantities obtained in step 2.

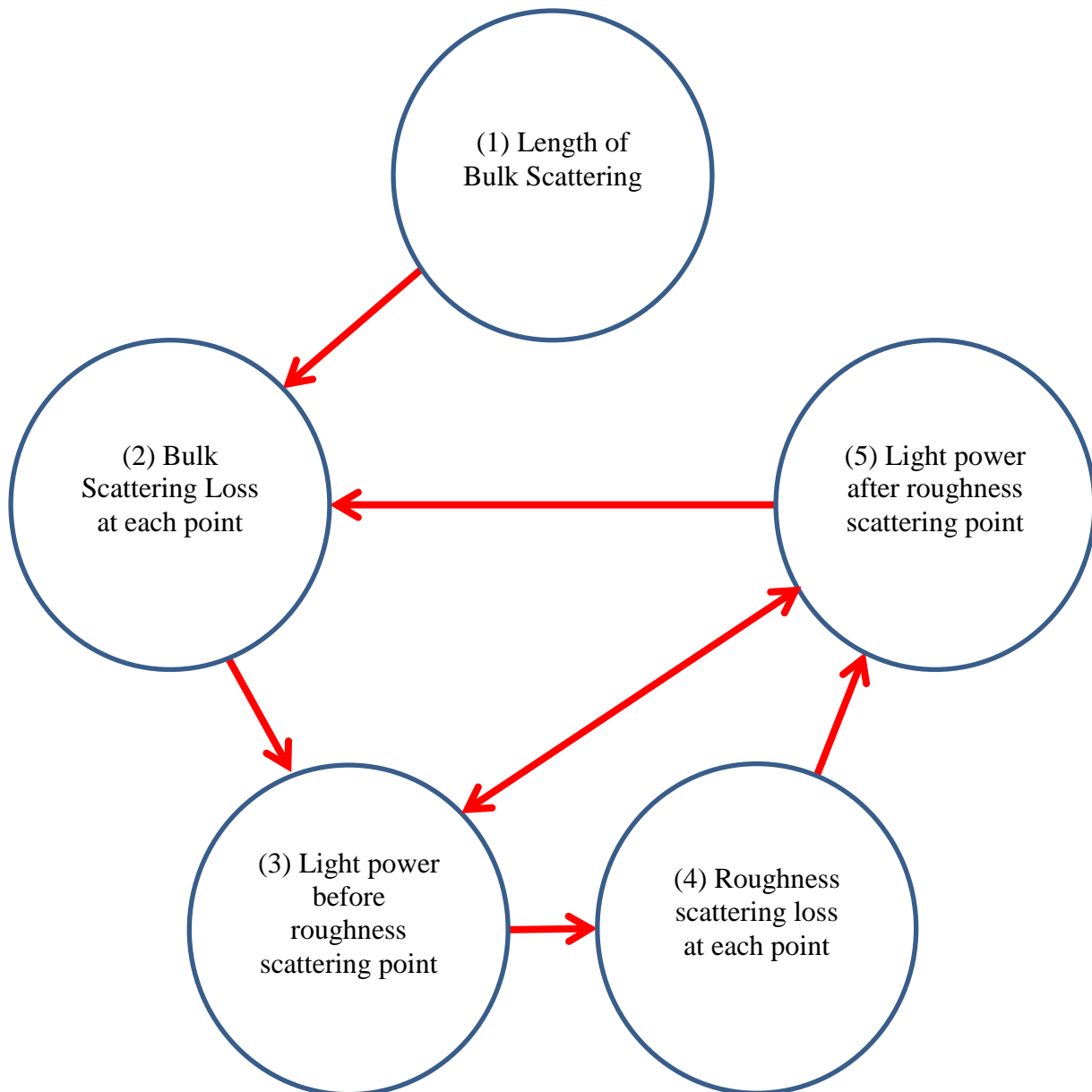


Figure 3.3: The relationship chart between each step of the process used in the analysis model and experimental comparison

Once all unknown values have been found from the self-consistent iterative process the transmitted light power calculation can be made as described in Eq. (3.1). When a laser beam is traveling within the specimen, there are two Fresnel reflection losses, surface roughness

scattering loss depending on the incident angle, and bulk scattering loss with absorption loss. If the reflection angle is not changed in the specimen, the ratio of the Fresnel loss at the incident surface is the same as the loss at the exit surface. The ratio of roughness scattering and the ratio bulk scattering with absorption are described by the TIS and the Beer-Lambert Law. Based on this ratio, the transmitted light power is determined by Eq. (3.1) as shown in Table A.2.

The amount of the refracted light is decreases proportionally with light propagation distance and these losses are analyzed by Eq. (2.6) which is considered scattering by particle and intrinsic absorption. As the laser beam travels through the material, total internal reflection occurs at the each surface boundary, however, the light wave also losses energy because of surface roughness scattering. This loss can be described by the TIS model. Lastly, when the light beam exits the material, Fresnel reflection occurs again. Because the refractive index and transmitted angle have not changed, the Fresnel reflection loss ratio is the same as the first surface. Thus, the output power can be calculated using previous step results.

In order to verify the calculations, the sum of transmitted light, absorption loss, scattering losses, and reflection loss has to be '1' because of energy conservation. This assures us that the light analysis model accounts for all energy lost by scattering and reflection. Each of the losses that contribute to the total light loss is calculated using the table shown in Table A.1 and summarized in Table A.3.

After all model calculations are finished, the last process is to find the surface roughness value using the 'solver' function in Excel. Through the 'solver' function, we can find the surface roughness RMS value which has the smallest sum of errors as shown in Table A.4. The difficulty

in exactly predicting the loss is that the light is spreading due to diffraction especially at high incident angles as shown in Fig.3.1. Thus, experimental data was only considered for trials for incident angles between 0 degree to 20 degree. However, the analysis model can be applied for higher incident angles depending on material condition and amount of light propagation as long as the calculation results look very similar to the experimental results.

This analysis model was also coded using a Matlab program, as shown in Appendix B. The Matlab program is also separated into parts such as Fresnel reflection loss ratio, roughness surface scattering loss ratio, bulk scattering ratio, and second Fresnel reflection loss ratio like the analysis model in Excel. The transmitted power is also calculated by Eq. (3.1). After that, the roughness RMS value can be determined by finding to quantity which satisfies the minimum difference between experimental results and calculation results. The roughness values from Matlab and Excel are slightly different because of the different solver procedures. However, all roughness values were consistent.

4. Experiments

In the previous chapter, a model was developed for light loss in an optical light pipes using surface roughness and other parameters. This chapter will describe the required experiments that apply this specific analysis model. Besides the surface roughness value, the analysis model requires other physical variable values including specimen size, specimen refractive index, laser wavelength, mean free path, the ratio between input and output power measured from experiment. Most variable values except the mean free path and the ratio between input and output are known. There are two different experiments required in order to find these two unknown values. One is measuring light power prior to entering a specimen and after exiting a specimen and another is measuring transmitted light power for each different propagation length assuming the mean free path. All light exhibits diffraction during propagation in any medium.

Also, the longer the distance that the laser beam travels in the specimen, the more it spreads out into higher angles because of surface reflection and small particle scattering. The diameter that is size of the laser beam as it reaches the exit surface is higher than the beam's initial size. An integrating sphere was used to collecting all of the light as it spread by diffraction and scattering. In this research, we used the integrating sphere with radiometer (Labsphere Model LM-4000).

In order to verify the analysis model, we compared the surface roughness RMS value obtained from the analysis model based on experimental results and the results from other

surface roughness measurements. An AFM (Atomic Force Microscope) and New View Zygo interferometer are used to find the surface roughness of the test samples.

4.1 Experimental set-up and procedure for measuring incident light and transmitted light

The light source is a helium-neon (He-Ne) laser which is already polarized. The polarization angle influences the amount the Fresnel reflection losses that occur when the beam encounters a surface. In order to easily analyze the Fresnel reflection loss, the laser was aligned to emit s-polarized beam. For this experiment, a polarizing filter which passes s-polarized light was installed in front of the laser to maximize the power. The laser power was also controlled using a set of neutral density filters, as shown in Fig. 4.1. The specimen stage was set up in behind the neutral density filters about 15cm in order to measure incident light power and transmitted light power. The distance of 15cm allows sufficient space for installing integrating sphere.

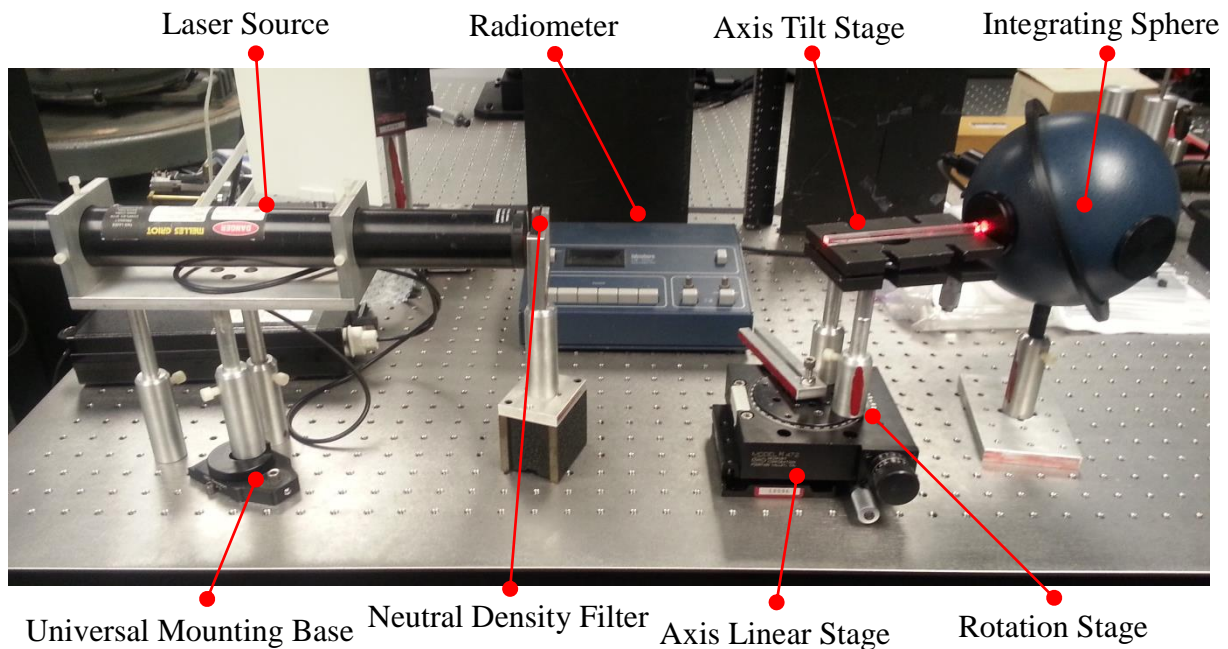


Figure 4.1: Experimental set up for applying to analysis model

The laser beam must enter the center of the incident surface of the specimen to conform to the initial conditions of the analysis model. Also, the universal mounting base was used on one of laser stages so that the beam could be aimed accurately on to the center of the incident surface in the specimen. An axis tilt stage and a linear stage were used for aligning the laser beam down the geometric the center of specimen. A rotation stage allows the incident angle to change with the end of the sample centered on its axis of rotation. After completing alignment, the integrating sphere can be placed at the exit surface of specimen to measure transmitted power.

To measure incident light power, the integrating sphere was installed between the neutral density filters and the specimen stage. For transmitted light power, the integrating sphere moves to the opposite exit surface of the specimen. The rotation stage was rotated from 0 degree to 50

degree at intervals of 5 degrees. The integrating sphere collects all of the transmitted light. The most critical part of the experiment is to position the integrating sphere to collect a maximum of detected light power. For example, the ratio of the transmitted light power divided by incident power is shown in Table 3.1 (b).

4.2 Experimental set-up and procedure for assuming mean free path

In the analysis model, one of the unknown variable values is the mean free path which can change depending on specimen condition. So, besides the previous experiment, another experiment is needed in order to calculate the mean free path of the specimens. As shown in Fig.4.2, the experiment is similar to the previous set up in that it uses He-Ne laser, neutral density filter, integrating sphere, radiometer and specimen stages in line.

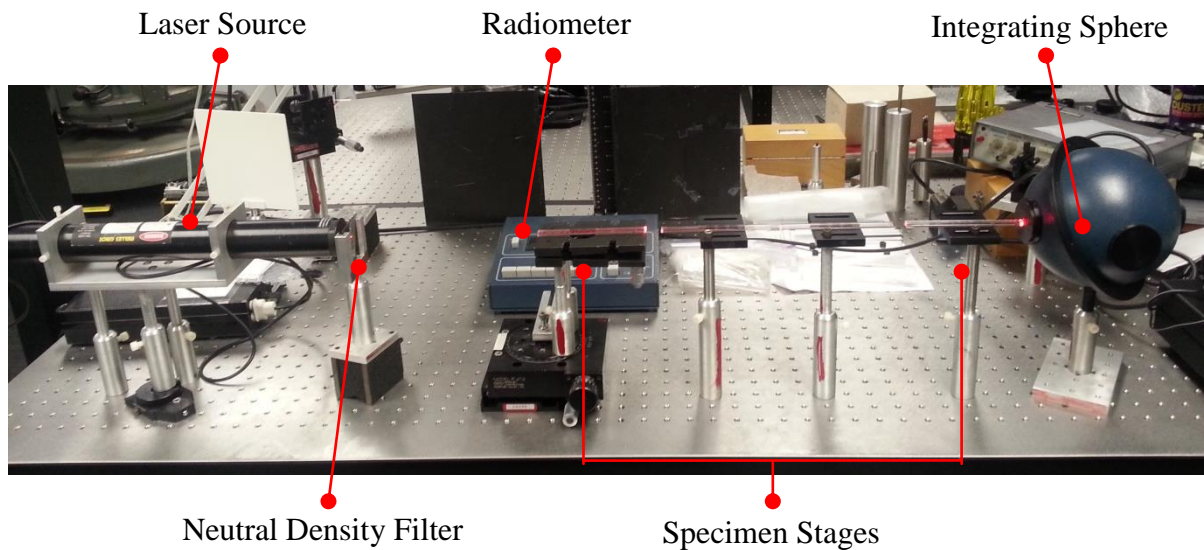


Figure 4.2: Experimental set up for determining mean free path

In this case, different lengths of specimens were fabricated of the same material and only the 0 degree incident propagation was used. Because there is no interaction at the side surfaces, surface roughness scattering is not a contributor to the transmittance. Eq. (2.6) and (2.15) summarize the analysis method used for these experiments,

$$T = e^{-\frac{x}{m}} \times (1 - R)^2 \quad (4.1)$$

$$\ln T = -\frac{1}{m} x + \ln(1 - R)^2 \quad (4.2)$$

Where T is transmitted light beam power, m is the mean free path, x is light propagation distance, m is the mean free path which is the reciprocal of attenuation coefficient and R is light loss coefficient consisting of Fresnel reflection coefficient and surface roughness scattering coefficient at the surface

In Eq. (4.2), $-\frac{1}{m}$ indicates the slope between x and $\ln T$ graph and $\ln(1 - R)^2$ shows y-intercept of the graph. Based on the data obtained through the experiment, we can fit this function to extract the needed parameters. Figure 4.3 shows two lines, one using a single specimen and the other using two specimens. For the case of two specimens, the y-intercept is shifted by $\ln(1 - R)^4$ because surface reflection occurs two times more than using a single specimen. The results of these experiments will be discussed in more detail in the next chapter.

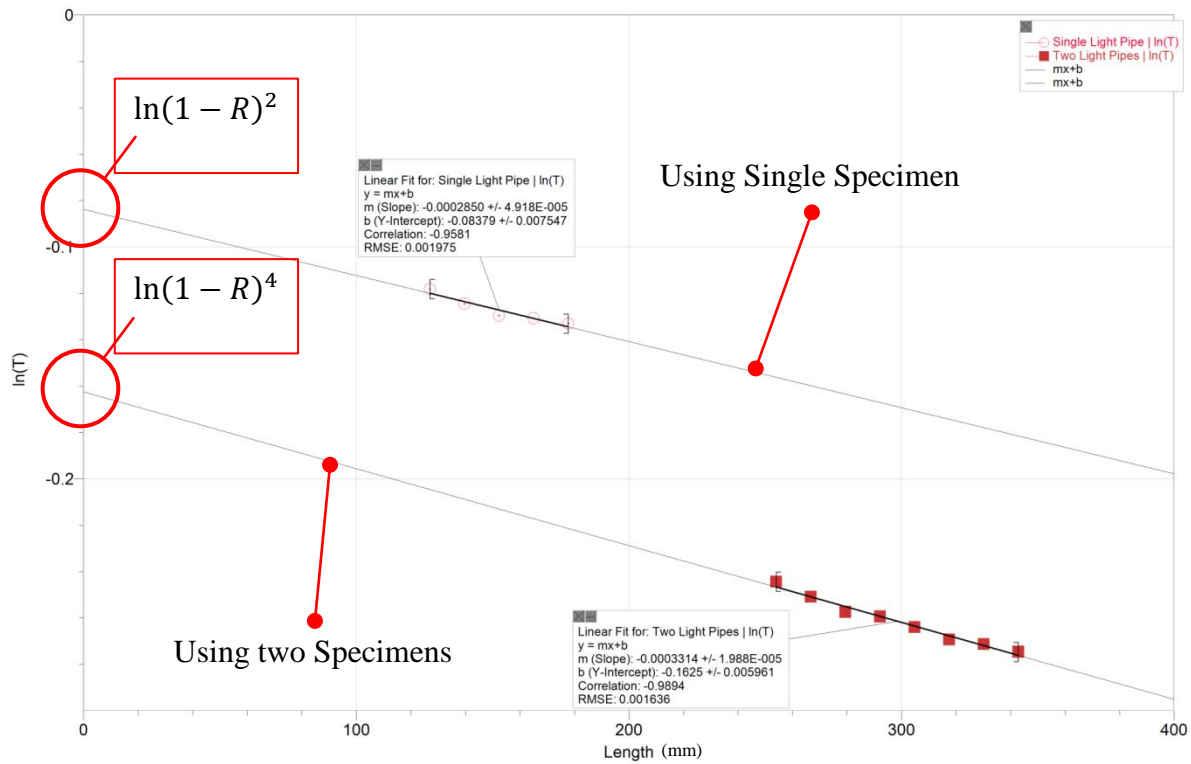


Figure 4.3: The graph of the experimental results to measure mean free path. The graphs indicate the natural logarithm of the transmittance versus total length of the specimen. In the experimental results using single specimen and using two specimens, five and eight experimental results are used for calculate the mean free path

Unfortunately, for one set of light pipe samples, we only had specimens of one length. In this case, we have to use two or more specimens at the same time in order to obtain data to determine the mean free path. Also, this process is a little complicated because the more specimens that are used, the more the numbers of reflections occur at the surface. In this case, the equation is expressed as follows,

$$\ln T = -\frac{1}{m} x + \ln(1 - R)^{2n} \quad (4.3)$$

Where n is the number of specimens which are all the same length.

The process used to extract the mean free path for samples of the same length is described below. As shown in Fig. 4.4, points A and A' represent natural logarithms of transmitted light (T) for two data points which were obtained using the same length specimens. Point A is the data for the sample where two surface reflections occur. So, the slope of \overline{AD} and y-intercept at point D can be expressed as $-\frac{1}{m}$ and $\ln(1 - R)^2$ such as before. That means if coordinate point A and point D are known, the mean free path can be calculated.

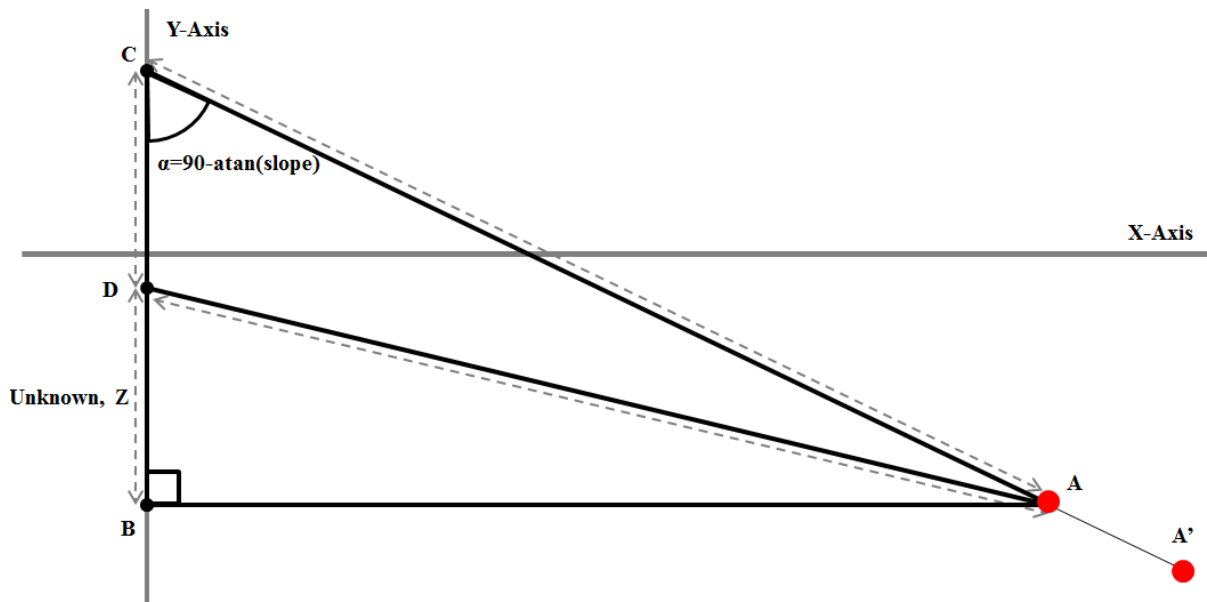


Figure 4.4: Schematic diagram illustrating the geometrical analysis used for same length specimens

When two or more of the same length light pipes are used the transmittance data results in a general point A', connecting A and A' leads to a new intercept at C. Now all information about \overline{AC} , coordinates of point A, point B, and point C are known. If length of \overline{BD} is assumed as an unknown variable 'Z', \overline{AD} and \overline{CD} can be expressed as shown in Fig. 4.4. From the triangle \overline{ACD} , we can find the triangle side length through cosine 2nd law because the lengths of

the sides of the triangle \overline{ACD} now can be expressed using one unknown value 'Z' and an angle at point C. Based on 'Z' obtained by calculation using cosine 2nd law, we can find coordinate point D and an equation which passes through point A and point D. As previously stated, $-\frac{1}{m}$ and $\ln(1 - R)^2$ are known through the equation,

$$C^2 = A^2 + B^2 - 2AB\cos(\alpha) \quad (4.4)$$

Where A, B, C are lengths of the sides and $\alpha=90-\tan^{-1}(\text{slope})$

In both processes, either using different length specimens or using specimens of the same length, the mean free path and reflection loss coefficient occurring at incident surfaces and exit surfaces are calculated. The reflection loss coefficient includes Fresnel reflection loss coefficient and roughness surface scattering loss coefficient

The experimental procedure for measuring mean free path with multiple specimens is similar to the previous experiment for measuring transmitted light power. As before, the integrating sphere is installed on the opposite exit surface of the specimen and detects the maximum transmitted light power. Whenever the specimens are added, the specimen stages are also added and the measurement method is the same as the previous process.

The most critical part of this experiment is to install the specimens at intervals along the laser propagation direction. Figure 4.5 indicates how the specimens are installed for three different types: (a) Single specimen, (b) Multi-specimen (contact), and (c) Multi-specimen (Non-contact). If the specimens contact other specimens such as Fig. 4.5 (b), the Fresnel reflection losses and roughness scattering occurred at boundary between different medium does not happen between the specimens. Even if Fresnel reflection and roughness scattering occurs, the reflected

light and the scatter light are reflected again on the past specimens and this phenomenon makes it difficult to predict how much light power enters the specimen. So, the specimens are placed about at least 1cm apart on the stages in order to prevent a returning reflected light beam and scattered light beam.

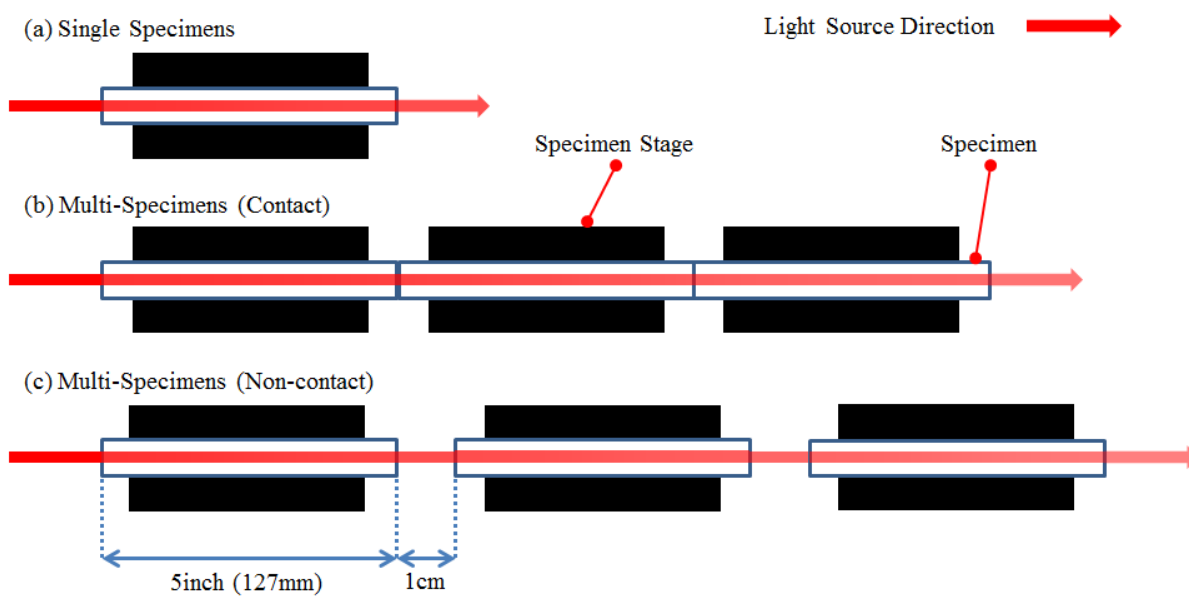


Figure 4.5: The top view of the experiment for measuring the mean free path using single and multiple PMMA light pipes

4.3 Other methods for measuring surface roughness

Side surface roughness of the specimen can be calculated through the analysis model applied by the experimental results from previous experiments. In order to determine how much the calculated surface roughness values compare with an independent measure of the surface roughness values, we used two other surface roughness measurements. These instruments are: 1)

New View Zygo [23] interferometer which analyzes roughness based on surface scan data and 2) type of AFM [24] which shows surface condition using a tip.

As shown in Fig. 4.6 (a), the New View Zygo interferometer provides high resolution, non-destructive, non-contact, 3D surface measurements utilizing the principles of Michelson interferometer and Mirau interferometer [23]. It shows 2D and 3D graphic images and high resolution numerical analysis of the surface structure of the specimen. In particular, this system can measure small structures and topography of specimen surfaces using white light interferometry without contacting the surface. In this research, a 10X Mirau objective lens and a 20X Mirau objective lens were used for the Mirau interferometer. For the case of high reflective surfaces such as mirrors and very smooth polished metal, the measurement cannot scan the surface structures because of the difficulty in detecting fringe patterns. For these situations, the surfaces must be measured by AFM which does not depend on reflections from the surface under test.

In Fig. 4.6 (b), atomic force microscopy (AFM) [24] is frequently used in area of research as a type of scanning probe microscopies which have very high resolution. It consists of a sharp probe tip which is used to scan the specimen surface. When the tip is moved to a region nearby the specimen surface, forces between the tip and the specimen occur which can be calculated from the deflection of the cantilever according to Hooke's law. By analyzing the deflection, the AFM output shows a 2D graphic image of the surface and the results of numerical analysis of the surface structure.

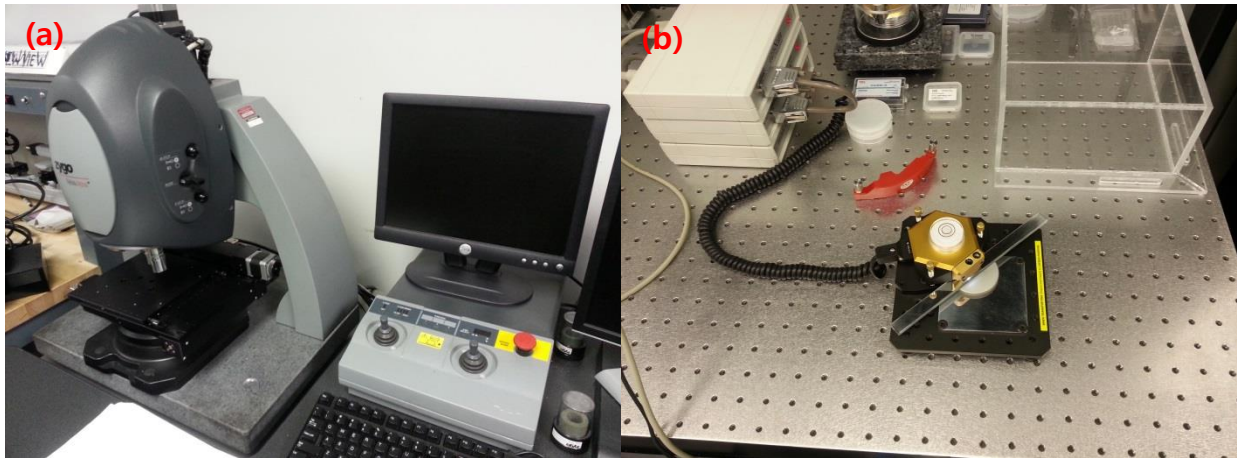


Figure 4.6: Surface roughness measurements (a) New View Zygo Interferometer (New View 6300), (b) Atomic Force Microscope (easyScan DFM)

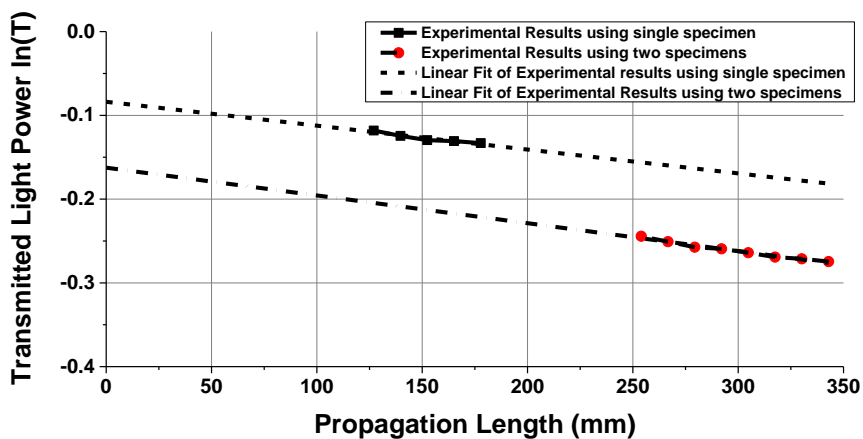
5. Results and Discussion

In the previous chapter, the analysis model and the experimental methods were described in order to calculate the surface roughness on the side of the specimen. This chapter discusses how the variables in the analysis model are obtained from experiment and how the surface roughness RMS values are calculated by the analysis model. Also, to verify the analysis model, the surface roughness results will be compared with results from roughness measurements using the AFM and the New View Zygo interferometer.

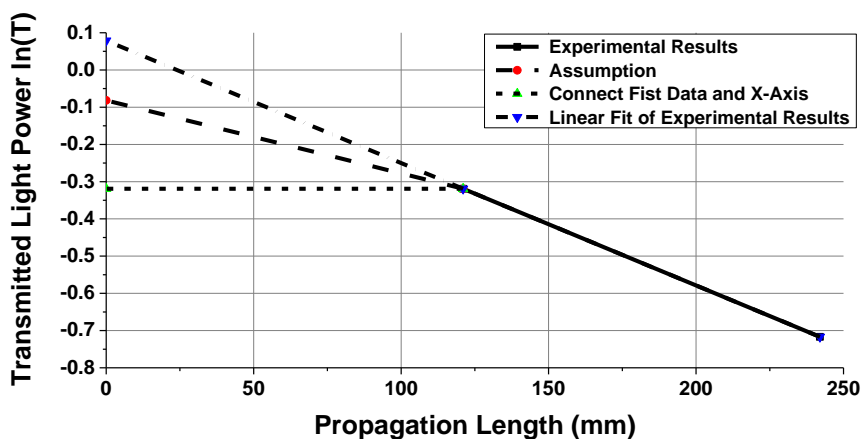
5.1 Results of the mean free path and reflection loss coefficient

The input values required for the analysis model are dependent on the specimen information; size, mean free path, refractive index, as well as the wavelength of laser source, and the transmitted light power. Of these, the mean free path must be determined by an experiment which is detailed in Chapter 4.2. For the case of the mirror and Al light pipes in which the light propagation paths are blanks, the bulk scattering loss is the same as the loss by diffusion in air. So, this information is only necessary when using solid light pipes.

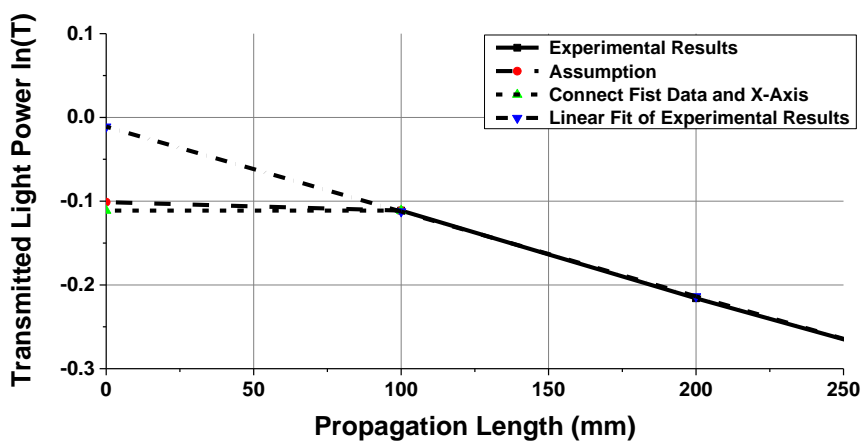
Figure 5.1 shows the results of the experiment for calculating the mean free path of the scattering within the bulk of glass light pipes, acrylic light pipes, and PMMA light pipes. For the glass light pipe and the PMMA light pipe, the mean free paths were determined using the method presented in Chapter 4.2 because we only had samples of a fixed length.



(a) Acrylic Light Pipe



(b) PMMA light pipe



(c) Glass Light Pipe

Figure 5.1: Experimental results to calculate the mean free path

Figure 5.2 shows results comparing the scattered light caused by bulk scattering in the specimen. A small value for the mean free path means that there are numerous small particles which cause bulk scattering and is the main contribution for the scattering loss in the specimen. In the PMMA light pipe, like the results of the previous experiments, bulk scattering dominates. On the other hand, the bulk scattering is small in the glass light pipe because that consists of pure material.

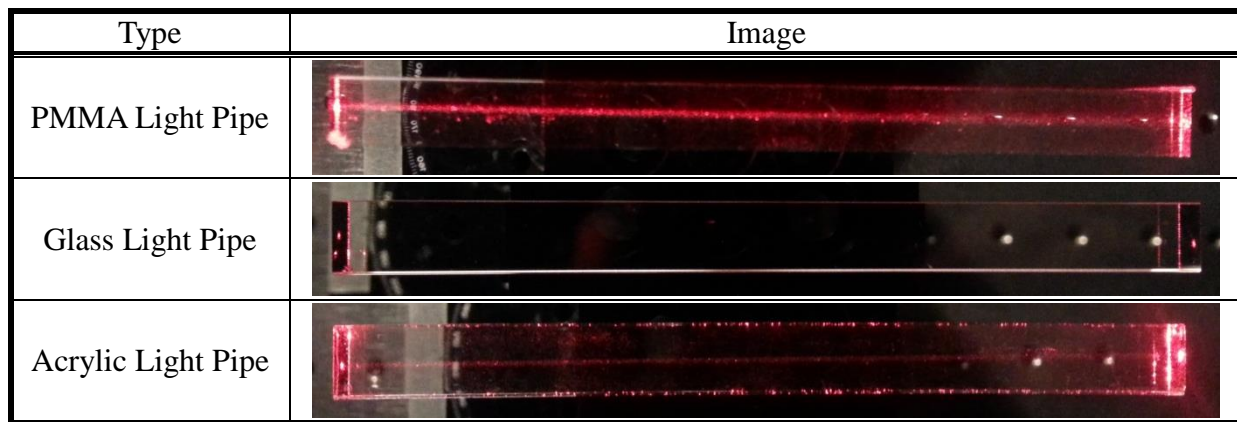


Figure 5.2: Comparing the amount of the light propagation for 0 degree incident angles

Table 5.1: The results of the mean free path and reflection loss coefficient

Type	Mean Free Path (μm)	Reflection Loss Coefficient
PMMA Light Pipe	509.4 μm	0.03994
Glass Light Pipe	8859.3 μm	0.04931
Acrylic Light Pipe	3017.5 μm	0.04103

The reflection loss coefficient includes the Fresnel reflection loss and the surface roughness scattering loss at the incident surface and the exit surface. When the light beam enters the specimen at 0 degree incident angle, the Fresnel reflection loss is influenced by the refractive

index of the specimen. The PMMA light pipe and the acrylic light pipe have similar values of refractive index (1.4815 and 1.4903 respectively) [25]. From the experimental data, we find that the surface roughness of the acrylic light pipe is higher than the surface roughness of the PMMA light pipe at the incident surface and the exit surface. Also, for the case of the glass light, whose surfaces are well polished, the reflection loss coefficient is the highest because the refractive index of glass is larger than the other specimens

5.2 Calculate the surface roughness RMS value

Using the experimental procedures introduced in Chapter 4.1, measurement of the transmitted light and incident light allows the mean free path to be determined as required by the analysis model. The values of the mean free path obtained by the experiment are listed in Table 5.1. Using the ‘Solver’ function in Excel, the surface roughness RMS can be calculated from the analysis model. In this process, it is important that the experimental results within a defined range of incident angles only be used. The experimental results tend to be bigger than the model calculation results at high incident angle because the integrating sphere detects the surface roughness scattering light and bulk scattering light as well as the transmitted light. When the incident angle is lower than 25 degree or the number of total internal reflections in the specimen is under four, the light beam can be identified clearly. (See Figure 3.1 from an earlier chapter) So, we only used the experimental data obtained between 0 degree incident angle and 25 degree.

Figure 5.3 compares the calculated results and the experimental results for all test samples. In each graph, the dotted lines indicate transmitted light power calculated by the

analysis model and lines connecting the square data points show the experimental results. A characteristic of all the graphs for the solid medium specimens shows that the measured transmitted light power tends to decrease quickly until the incident angle reaches 20 degree and then decreases more slowly. This phenomenon occurs because of light loss in the specimen caused by the bulk scattering and the surface roughness scattering entering into the integrating sphere.

Rough surfaces tend to decrease the transmitted light power significantly such as the difference between the acrylic light pipe fabricated by the laser cutting and well-polished acrylic light pipe. (See Figure 5.3 and Figure 5.5) In the glass light pipe, there is no major loss even though the incident angle is increasing because it is a pure material and polished well. However, the bulk scattering and the surface roughness scattering in the PMMA light pipe occur more than in other solid light pipes because these samples also include small particles. For the case of the mirrored guides, there are three different experiment conditions: 1) two well-polished mirrors, 2) one well-polished mirror with a polished mirror for 15min. and 3) one well-polished mirror with a polished mirror for 45min. As was expected, the more the mirror is polished, the less the transmitted light power is detected.

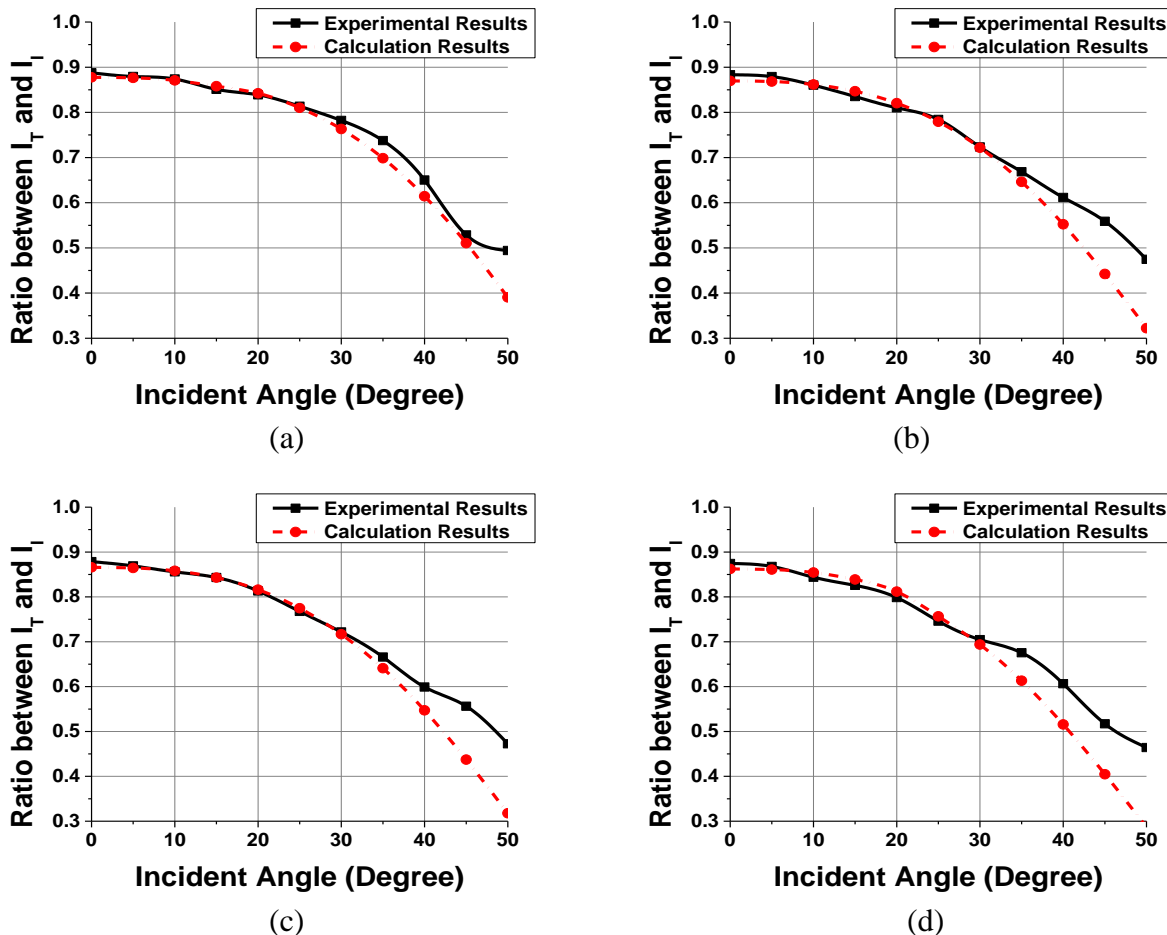


Figure 5.3: the graphs of comparing the experimental results and the calculation results: well-polished acrylic light pipe (a) 5.5 inch, (b) 6 inch, (c) 6.5 inch, and (d) 7 inch

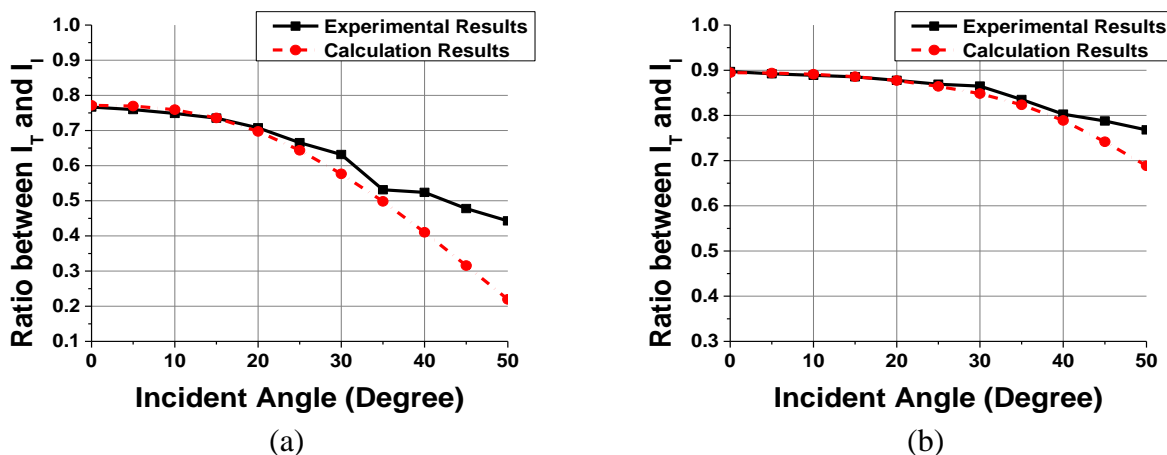


Figure 5.4: Comparison between the experimental results and the calculation results: (a) PMMA light pipe (5 inch) and (b) Glass light pipe (10cm)

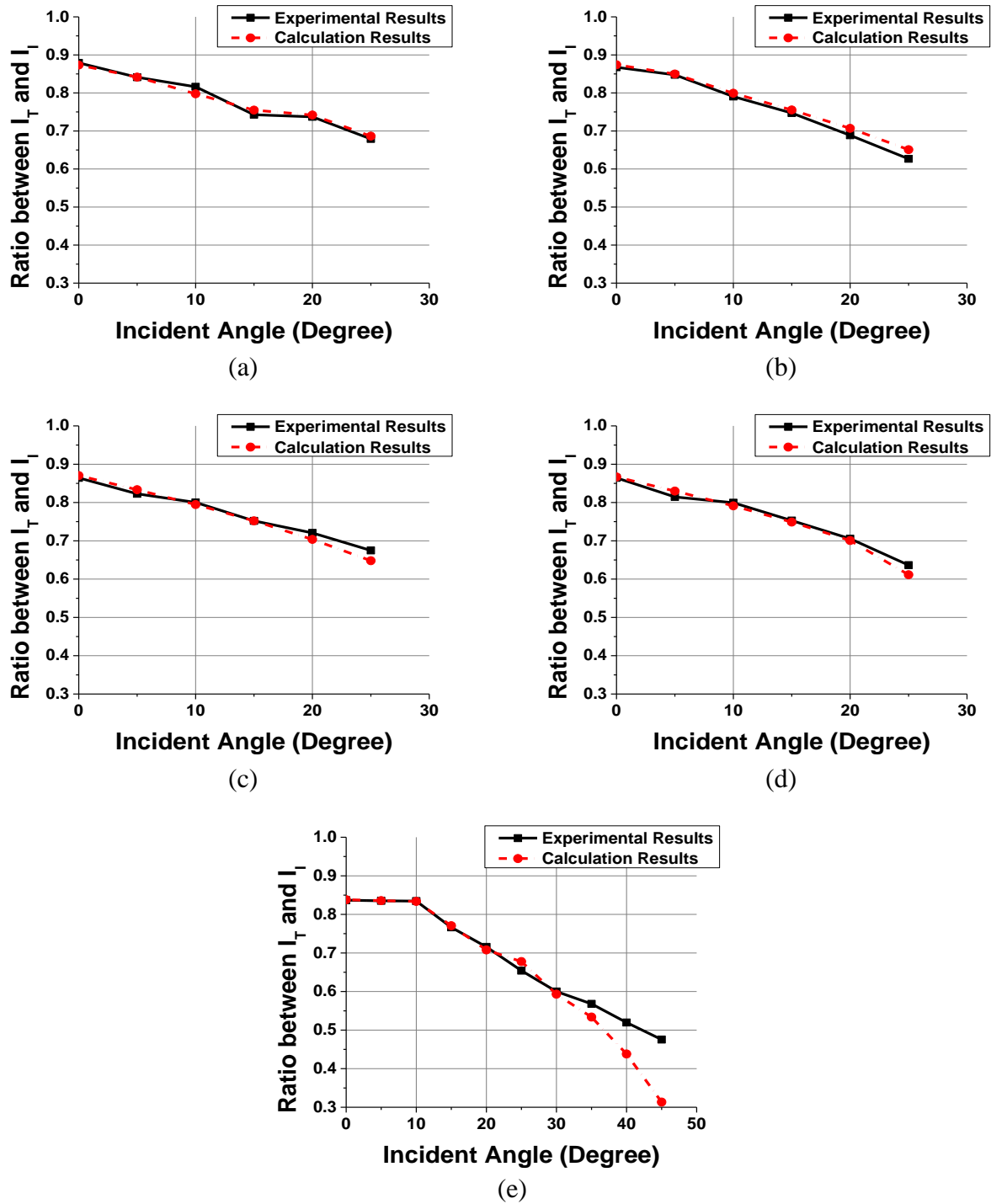
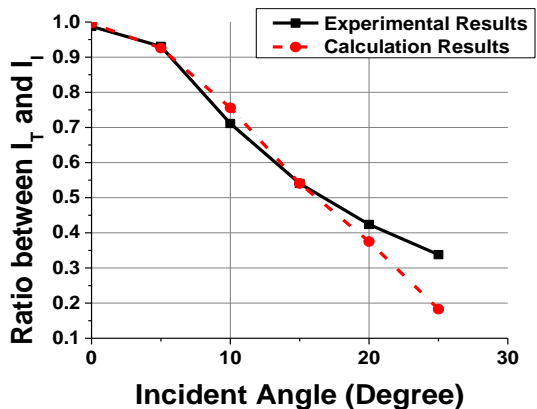
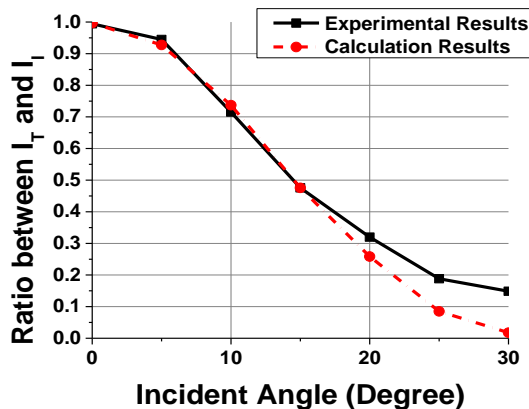


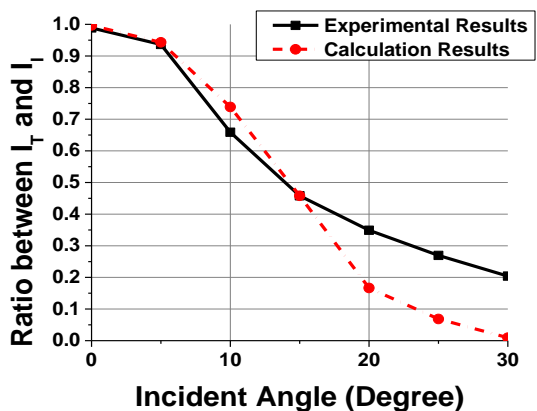
Figure 5.5: Comparison of the experimental results and the calculation results: Acrylic light pipe fabricated by laser (a) 5.5 inch, (b) 6 inch, (c) 6.5 inch, and (d) 7 inch and (e) Curved acrylic light pipe fabricated by laser



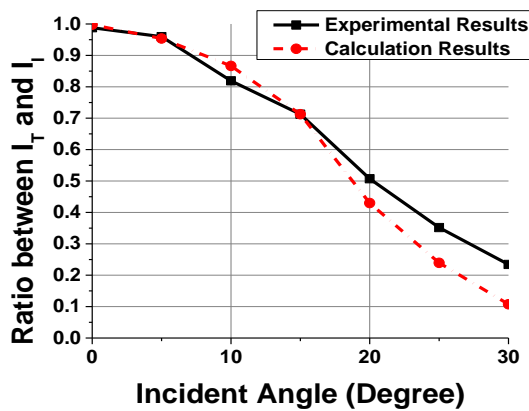
(a) Two well-polished mirrors (6 inch)



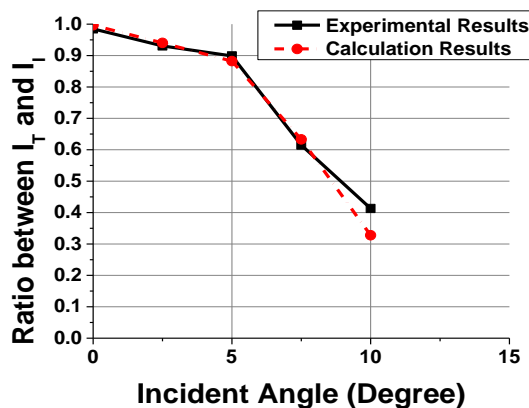
(b) Good condition mirror with a polished mirror for 15 min (6 inch)



(c) Good condition mirror with a polished mirror for 45 min (6 inch)



(d) Well-polished Al light pipe (10 cm)



(e) Al light Pipe fabricated by milling (6 inch)

Figure 5.6: Comparison of the experimental results and the calculation results: (a) PMMA light pipe (5 inch) and (b) Glass light pipe (10cm)

Table 5.2 summarizes the results of all surface roughness values calculated by the analysis model. The well-polished acrylic light pipes were fabricated using a similar method and their roughness values are very similar to each other at around $0.074\mu\text{m}$. However, the results of the acrylic light pipe fabricated by laser cutting show very large roughness values because their surface roughness are larger than the light wavelength. The PMMA light pipe has $0.151\mu\text{m}$ surface roughness. When the mean free path of the glass light pipe was applied to the analysis model, we obtained a zero surface roughness value. Through analysis of the amount of light loss inside the glass light pipe at an incident angle of 0 degree, we compute a new mean free path value ($15,233\mu\text{m}$). The surface roughness RMS of the glass light pipe is $0.0215\mu\text{m}$ and it is the smoothest among the specimens. For the mirror, as was expected, the more the surface was polished with various grits, the larger the surface roughness values. The Al light pipe which was not polished after fabrication using a milling process has high surface roughness RMS.

Table 5.2: A summary of all the results of surface roughness calculated by the analysis model

Medium	Material	Surface condition	Specimen Length	Calculation Results (μm)
Solid	Acrylic	Well-Polished	139.7cm (5.5 inch)	0.073
Solid	Acrylic	Well-Polished	152.4cm (6 inch)	0.075
Solid	Acrylic	Well-Polished	165.1cm (6.5 inch)	0.074
Solid	Acrylic	Well-Polished	177.8cm (7 inch)	0.075
Solid	Acrylic	Laser Cutting	139.7cm (5.5 inch)	0.803
Solid	Acrylic	Laser Cutting	152.4cm (6 inch)	0.589
Solid	Acrylic	Laser Cutting	165.1cm (6.5 inch)	5.800
Solid	Acrylic	Laser Cutting	177.8cm (7 inch)	10.600
Solid	Acrylic (curved)	Laser Cutting	165.1cm (6.5 inch)	Over 10
Solid	PMMA	Well-Polished	127cm (5 inch)	0.151
Solid	Glass	Well-Polished	10cm	0.022
Air	Mirror	Well-Polished	16cm	0.046
Air	Mirror	Polished by 300nm aluminum abrasive for 15min	16cm	0.076
Air	Mirror	Polished by 300nm aluminum abrasive for 45min	16cm	0.167
Air	Al	Well-Polished	10cm	0.075
Air	Al	Milling	152.4cm (6 inch)	0.167

5.3 The surface roughness measured by other measurements

In order to verify the surface roughness RMS calculated by the analysis model, we used the AFM and the New View Zygo interferometer which provide both surface profile as well as measured values of the surface roughness. The acrylic light pipe, the PMMA light pipe, and the glass light pipe were measured by the New View Zygo interferometer because they do not have a highly reflective surface. The highly reflective mirror and Al light pipe surface roughness values were estimated from tests using the AFM. The surface roughness was measured 10 arbitrary positions on the specimen and the resulting value was calculated from the arithmetic mean. The experimental results are summarized at Table 5.3.

Table 5.3: Experimental results of surface roughness measured by AFM and New View Zygo interferometer

Medium	Material	Surface condition	Specimen Length	Calculation Results (μm)
Solid	Acrylic	Well-Polished	139.7cm (5.5 inch)	0.067 \pm 0.004
Solid	Acrylic	Well-Polished	152.4cm (6 inch)	
Solid	Acrylic	Well-Polished	165.1cm (6.5 inch)	
Solid	Acrylic	Well-Polished	177.8cm (7 inch)	
Solid	Acrylic	Laser Cutting	139.7cm (5.5 inch)	1.163 \pm 0.562
Solid	Acrylic	Laser Cutting	152.4cm (6 inch)	0.894 \pm 0.297
Solid	Acrylic	Laser Cutting	165.1cm (6.5 inch)	1.105 \pm 0.395
Solid	Acrylic	Laser Cutting	177.8cm (7 inch)	1.161 \pm 0.674
Solid	Acrylic (curved)	Laser Cutting	165.1cm (6.5 inch)	1.006 \pm 0.276
Solid	PMMA	Well-Polished	127cm (5 inch)	0.095 \pm 0.004
Solid	Glass	Well-Polished	10cm	0.018 \pm 0.001
Air	Mirror	Well-Polished	16cm	0.042 \pm 0.001
Air	Mirror	Polished by 300nm aluminum abrasive for 15min	16cm	0.079 \pm 0.014
Air	Mirror	Polished by 300nm aluminum abrasive for 45min	16cm	0.092 \pm 0.003
Air	Al	Well-Polished	10cm	0.066 \pm 0.001
Air	Al	Milling	152.4cm (6 inch)	0.334 \pm 0.023

5.4 Error analysis

Table 5.4 compares the surface roughness values obtained from the analysis model and the roughness tests. For the acrylic light pipe, the PMMA light pipe, and the glass light pipe, which are well polished, the calculation results are all on the order of 10% higher than the measurement results. As mentioned earlier, the analysis model is applicable only in the samples that have a surface roughness which is smaller than the light wavelength. So, the calculation results of the acrylic light pipe fabricated by laser cutting shows surface roughness values well over $1\mu\text{m}$ which may simply show that this surface is not consistent with the model assumptions.

Table 5.4: Summary of the results of surface roughness RMS including experimental error and differences between the model calculations and experimental values

Medium	Specimen Length	Results from Analysis model (μm)	Results from measurements (μm)	Error (%)	Difference (μm)
Acrylic	139.7cm (5.5 inch)	0.073	0.067 \pm 0.004	8.36%	0.006
Acrylic	152.4cm (6 inch)	0.075		10.74%	-0.002
Acrylic	165.1cm (6.5 inch)	0.074		9.96%	-0.136
Acrylic	177.8cm (7 inch)	0.075		11.16%	-0.015
Acrylic	139.7cm (5.5 inch)	0.803	1.163 \pm 0.562	-44.89%	0.361
Acrylic	152.4cm (6 inch)	0.589	0.894 \pm 0.297	-51.77%	0.305
Acrylic	165.1cm (6.5 inch)	5.800	1.105 \pm 0.395	80.94%	-4.695
Acrylic	177.8cm (7 inch)	10.600	1.161 \pm 0.674	89.05%	-9.439
Acrylic (curved)	165.1cm (6.5 inch)	Over 10	1.006 \pm 0.276	-	-
PMMA	127cm (5 inch)	0.151	0.095 \pm 0.004	17.65%	-0.020
Glass	10cm	0.022	0.018 \pm 0.001	15.81%	-0.001
Mirror	16cm	0.046	0.042 \pm 0.001	9.93%	-0.005
Mirror	16cm	0.076	0.079 \pm 0.014	-3.81%	0.003
Mirror	16cm	0.167	0.092 \pm 0.003	45.21%	-0.075
Al	10cm	0.075	0.066 \pm 0.001	12.46%	-0.009
Al	152.4cm (6 inch)	0.167	0.334 \pm 0.023	-99%	0.167

For the two different air guided specimens which use mirrors and Al light pipes, the calculated roughness value is almost 10% greater than the measurement results as with the well-polished other specimens. But, in the case of the mirrors polished by a 300nm aluminum abrasive, the calculated results of the mirror polished for 15 minutes are quite similar with the measurement results and the calculated value and was 45% greater than the measurement results using the mirror polished for 45 minutes. This large difference is probably due to the uneven surface polish. Also, numerous large and small scratches lead to unexpected problems because the mirror was polished by hand without a mechanical device.

As shown in Fig. 5.7, the ratio between the calculation results and the measurement results of the well-polished Al light pipe is around 10% like the other well-polished specimen. Although the surface roughness of the Al light pipe which was not polished after milling is lower than the light wavelength, the measurement results is almost two times larger than the calculated results. As shown in Fig. 5.8, the scattered light at the side surface also exits out with the transmitted light because of the surface including milling marks. Thus, the integrating sphere collects this scattered light as well as the transmitted light. This leads to an over estimation for the input data as applied to the analysis model resulting in a less than actual value obtained.

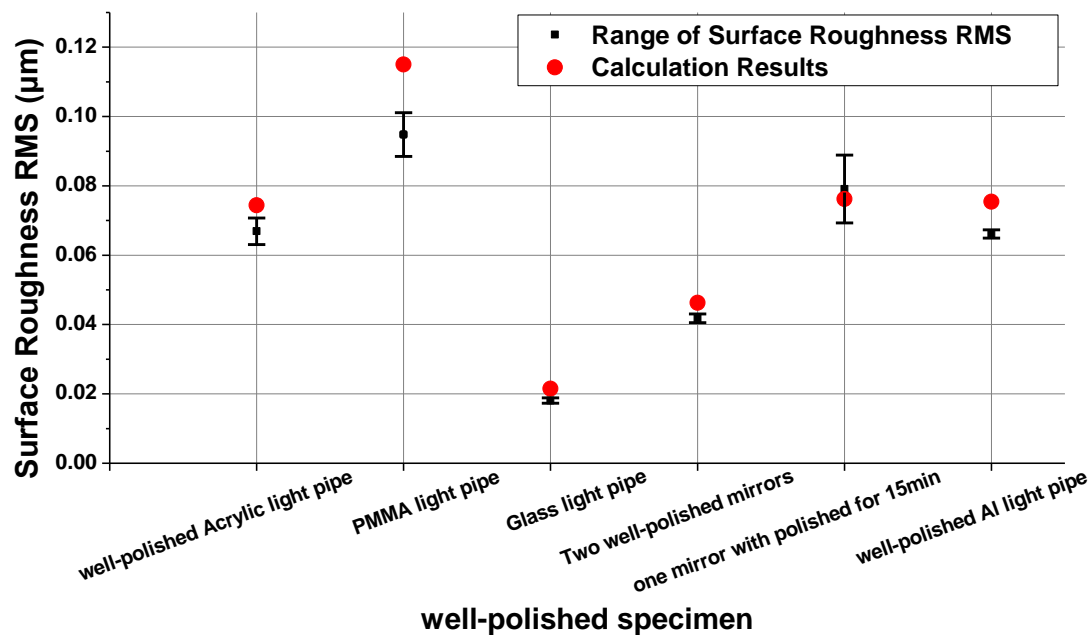


Figure 5.7: Comparing the calculation results and range of surface roughness RMS when using well-polished specimen

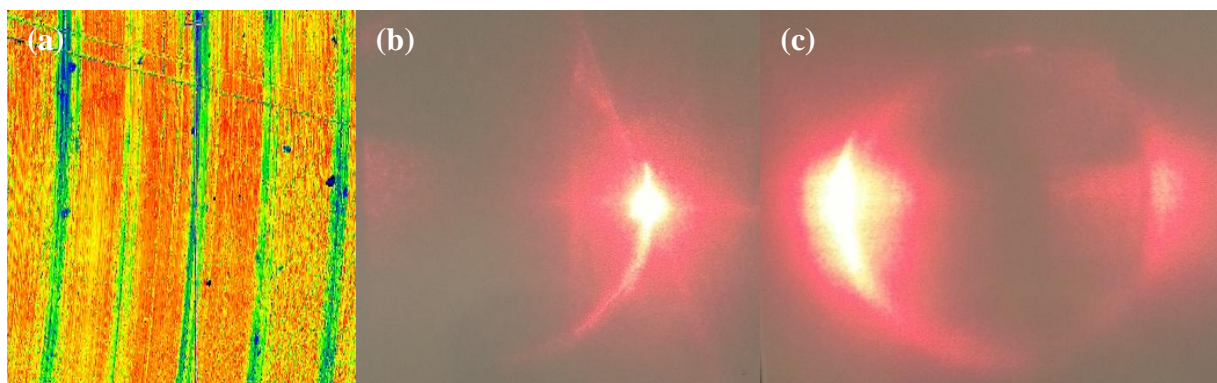


Figure 5.8: (a) the surface profile of Al light pipe fabricated by milling, (b) Shape of the transmitted light pattern at 10 degrees in the well-polished Al light pipe, and (c) similar pattern for the Al light pipe fabricated by milling.

6. Conclusions and Future work

This thesis describes the characteristics of scattering loss and absorption loss in a variety of optical light pipe configurations. In order to analyze light propagation in the light pipes, an analysis model was developed to consider all light loss mechanisms. In particular, the analysis model focused on the loss caused by surface roughness and how the surface roughness can be calculated using this model along with experimental results. Both an AFM and New View Zygo interferometer were also used for verify the surface roughness calculated by the analysis model.

The specimens tested were a combination of solid- and hollow-core light pipes having different specimen length, medium, surface roughness, and embedded particles. In order to apply this model, the specimen must satisfy the following conditions. The first condition is that the surface roughness RMS value of the specimen should be smaller than the wavelength of the light source. The second condition is that the surface of the specimen must be polished.

Comparing the results of the analysis model and measurement as that shown in Table 5.4, we can conclude that the results of the analysis model were of the order of 10% higher than the measurement results for well-polished specimens which satisfy the two conditions applied to the analysis model. However, for the case of the specimens that were not well polished, the analysis model predicts a large roughness value compared to the measurement results because the TIS equation used in the analysis model assumes that the roughness is of the order of the wavelength of light. The results of the specimen satisfied only the second condition show that calculated results are half of actual roughness because of unexpected scattering occurs at the rough surface.

A curved light pipe was also fabricated using a laser cutting process, but it could not be applied to this model because of its high surface roughness. Various shapes of light pipes that are

well-polished could be tested using the methods developed. More work is needed in order to analyze specimens which have a roughness bigger than the wavelength.

LIST OF REFERENCES

- [1] David L. Andrews, Perspectives in Modern Chemical Spectroscopy, springer-verlag Berlin Heidelberg, New York
- [2] The physics classroom, Light absorption, reflection and transmission, viewed 13 June 2016, <http://www.physicsclassroom.com/class/light/Lesson-2/Light-Absorption,-Reflection,-and-Transmission>
- [3] West, Willia, "Absorption of electromagnetic radiation", AccessScience. McGraw-Hill (2014)
- [4] Youl-Ki Choi, "The optical properties absorption PMMA color filters doped with Neodymium ions", M.S. Thesis, Kyungpook National University, (2004)
- [5] M. Kerker, "The scattering of light and other electromagnetic radiation", Academic, New York, (1969)
- [6] H.C. van de Hulst., Light scattering by small particles, Dover Publications, New York, (1981)
- [7] C.F. Bohren and D.R. Huffman., Absorption and scattering of light by small particles. John Wiley & Sons, New York, (1983)
- [8] Jae Joon Choi, "An Experimental Study on the Single Vortex Ring using Rayleigh scattering Method", M.S. Thesis, Korea Advanced Institute of Science and Technology, (1998)

- [9] Anthony B. Davis and Alexander Marshak, "Photon propagation in heterogeneous optical media with spatial correlations: enhanced mean-free-paths and wider-than-exponential free-path distributions", *J. Quantitative Spectroscopy & Radiative Transfer*, Vol. 84, Issue 1, (2004)
- [10] James E. Harvey, Sven Schröder, Narak Choi, and Angela Duparré, "Total integrated scatter from surfaces with arbitrary roughness, correlation widths, and incident angles", *Opt. Eng.*, Vol. 51, Issue 1 (2012)
- [11] Bennett, H. E., and J. O. Proteus, "Relation between Surface Roughness and Specular Reflection at Normal incidence," *J. Opt. Soc. Am.* Vol51: 123-129 (1961)
- [12] Beckman. P., and Spizzichino, A, "The Scattering of Electromagnetic Waves form Rough Surfaces," A Pergamon Press Book, (1963)
- [13] H. Davies, "the reflection of electromagnetic radiation from a rough surface", *IEE*, Vol. 101, Issue 7 (1954)
- [14] Zheng Zhenrong, Zhou Jing and Gu Peifu, "Roughness characterization of well-polished surfaces by measurements of light scattering distribution", *Optica Applicata*, Vol. XL, No. 4, (2010)
- [15] C. J. Tay, S. H. Wang, C. Quan, and C. K. Ng, "Surface Roughness measurement of semiconductor wafers using a modified total integrated scattering model", *Optik* 113, No. 7 (2002)
- [16] J. T. Remillard, M. P. Everson, and W. H. Weber, "Loss mechanisms in optical light pipes", *Applied Optics*, Vol. 31, No. 34, (1992)

- [17] Marc J. Madou, *Manufacturing Techniques for Microfabrication and Nanotechnology* (3rd ed), CRC Press, New York, (2011)
- [18] Eckhardt Optics LLC, *Optical Scattering and Surface Roughness*, viewed 13 June 2016, <http://eckop.com/optical-scatter-2/optical-scattering-versus-surface-roughness>
- [19] Eugene Hecht, *OPTICS* (4th ed.), Addison Wesley, San Francisco, (2002)
- [20] Mi Kyung Park, “Study on polarization characteristics of the optical elements by Fresnel equation”, M.S. Thesis, Korea National University of Education, (2004)
- [21] Grant R. Fowles, *Introduction to Modern Optics* (2nd ed.), Dover Publications, New York, (1975)
- [22] Frank L. Pedrotti, S.J., Leno S. Pedrotti, *Introduction to optics* (3rd ed.), Prentice- Hall International, Inc. (2006)
- [23] Zygo Corporation, “NewView 6200 & 6300 Operating Manual”, February (2006)
- [24] Nanosurf Corporation, “easyScan DFM Operating Instructions”, Jan (2003)
- [25] G. Beadie, M. Brindze, R. A. Flynn, A. Rosenberg, and J. S. Shrik, Refractive index measurements of poly(methyl methacrylate) (PMMA) from 0.4-1.6 μ m, *Appl. Opt.* 54, F139-F143 (2015)

APPENDIX A: Analysis model in Excel

This appendix provides more details of the analysis model calculations described in Chapter 3.2. As shown in Fig.3.3, there are five different steps in the calculation procedure; (1) length of bulk scattering, (2) bulk scattering loss at each point, (3) light power before roughness scattering point, (4) roughness scattering loss at each point, and (5) light power after roughness scattering point. The analysis model calculates the amount of light loss in the order in which the loss occurs within the specimen. Table A.1 (1) shows the light propagation length between points where the surface roughness scattering happened. The first row means the points at which the surface roughness scattering is happened. For example, '1-2' in Table A.1 (1) described the distance from the first roughness scattering point to the second point.

Table A.1 (2) shows that the bulk scattering loss with absorption loss at each point as calculated using Eq. (2.6) based on the values of the propagation length from Table A.1 (1) and the light power after roughness scattering from Table A.1 (5). Each cell shows the bulk scattering loss that occurs between any two TIR segments. The total column lists the sum of the bulk scattering.

In Table A.1 (3), the light power before the reflection has happened at the side surface of specimen is computed. In other words, it is the power remaining from the previous process. It is calculated easily using data of the light power after roughness scattering loss from Table A.1 (5) and the bulk scattering loss from Table A.1 (2).

Table A.1 (4) contains the data of light loss by surface roughness scattering at each point. They are calculated by Eq. (2.7) based on the data at Table A.1 (3). Like step 2, the sum of the surface roughness scattering loss which occurs at the same incident angle indicates total light loss by surface roughness scattering loss.

Table A.1 (5) is designed for bulk scattering loss calculation and includes the data which is the light power after roughness scattering. The '0' and '1' columns data shows the light power after Fresnel reflection. So, they are indicated as initial light power minus Fresnel reflection loss. Like step 3, other values are calculated using data of the light power before roughness scattering from Table A.1 (3) and the roughness scattering loss from Table A.1 (4).

Table A.1: Calculation steps of the analysis model (Step (1): bulk scattering length, Step (2): Bulk scattering loss at each point, Step (3): light power before roughness scattering point, Step (4): roughness scattering loss at each point, and Step (5) Light power after roughness scattering)

(1) Incident Angle	0	0-1	1-2	2-3	3-4	4-5	5-6	6-7
0	121	-	-	-	-	-	-	-
5	-	67.993	53.217	0	0	0	0	0
10	-	34.126	68.253	19.460	0	0	0	0
15	-	22.896	45.793	45.793	8.408	0	0	0
20	-	17.326	34.653	34.653	34.653	3.074	0	0
25	-	14.022	28.044	28.044	28.044	28.044	0.047	0

(2) Incident Angle	0-0	0-1	1-2	2-3	3-4	4-5	5-6	6-7	Total
0	0.203	-	-	-	-	-	-	-	0.203
5	-	0.120	0.083	0	0	0	0	0	0.204
10	-	0.062	0.112	0.029	0	0	0	0	0.203
15	-	0.042	0.078	0.070	0.012	0	0	0	0.202
20	-	0.032	0.060	0.054	0.050	0.004	0	0	0.200
25	-	0.026	0.048	0.044	0.041	0.037	0.000	0	0.196

(3) Incident Angle	0	1	2	3	4	5	6	7
0	-	-	-	-	-	-	-	-
5	0.842	0	0	0	0	0	0	0
10	0.899	0.781	0	0	0	0	0	0
15	0.917	0.827	0.747	0	0	0	0	0
20	0.924	0.845	0.774	0.708	0	0	0	0
25	0.925	0.850	0.780	0.717	0.658	0	0	0

(4) Incident Angle	0	1	2	3	4	5	6	7	Total
0	0	-	-	-	-	-	-	-	0
5	0.002	0	0	0	0	0	0	0	0.002
10	0.008	0.007	0	0	0	0	0	0	0.016
15	0.017	0.015	0.014	0	0	0	0	0	0.046
20	0.027	0.024	0.022	0.020	0	0	0	0	0.093
25	0.036	0.033	0.030	0.027	0.025	0	0	0	0.151

(5) Incident Angle	0	1	2	3	4	5	6	7
0	0.962	-	-	-	-	-	-	-
5	0.962	0.841	0	0	0	0	0	0
10	0.961	0.893	0.777	0	0	0	0	0
15	0.959	0.905	0.817	0.738	0	0	0	0
20	0.956	0.905	0.828	0.758	0.694	0	0	0
25	0.951	0.898	0.825	0.757	0.695	0	0	0

Table A.2: Calculating transmitted light power with each loss coefficients

Incident Angle	Ratio of Fresnel Loss at incident surface	Ratio of Roughness Scattering Loss	Ratio of Bulk Scattering Loss	Ratio of Fresnel Loss at exit surface	Output Power
0°	0.038	0.000	0.211	0.038	0.730
5°	0.038	0.003	0.212	0.038	0.728
10°	0.039	0.009	0.213	0.039	0.713
15°	0.041	0.019	0.214	0.041	0.682
20°	0.044	0.029	0.217	0.044	0.636
25°	0.049	0.039	0.220	0.049	0.579
30°	0.055	0.049	0.223	0.055	0.540
35°	0.063	0.059	0.227	0.063	0.470
40°	0.073	0.072	0.232	0.073	0.392
45°	0.088	0.087	0.237	0.088	0.308
50°	0.107	0.107	0.242	0.107	0.219

The analysis model assumes that all energy losses are caused by scattering or reflection. So, the sum of transmitted light and scattering losses and reflection loss has to be '1'. There are five different ingredients; the transmitted light power and four different light losses. The values of the transmitted light power use calculated values in Table A.2. Amount of the light loss by Fresnel reflection at incident surface is same with the Fresnel reflection coefficient because initial light power is assumed '1' before the Fresnel reflection loss occurs. In the case of the bulk scattering loss and the roughness scattering loss, we use the calculated values in Table A.1 (2) and (4). When the light beam emerges from the specimen, the Fresnel reflection again occurs. It is calculated by using the following methods,

$$\begin{aligned}
 \text{Fresnel loss at exit surface} = & (1 - \text{First Fresnel Reflection Loss ratio}) \\
 & \times (1 - \text{Roughness Scattering Loss ratio})^n \\
 & \times (1 - \text{Bulk Scattering Loss ratio}) \\
 & \times (\text{Second Fresnel Reflection Loss ratio})
 \end{aligned} \tag{A.1}$$

As shown in Table A.3, we confirm the proper operation of the analysis model through the sum of the transmitted light power and four light losses.

Table A.3: Verify energy conservation in the analysis model

Incident Angle	Transmitted light Power	Fresnel Loss at incident surface	Bulk Scattering Loss	Roughness Scattering Loss	Fresnel Loss at exit surface	Total
0	0.730	0.038	0.203	0.000	0.029	1
5	0.728	0.038	0.203	0.002	0.029	1
10	0.713	0.039	0.203	0.016	0.029	1
15	0.682	0.041	0.201	0.046	0.029	1
20	0.636	0.044	0.197	0.093	0.030	1
25	0.579	0.049	0.192	0.151	0.030	1
30	0.540	0.055	0.186	0.188	0.031	1
35	0.470	0.063	0.178	0.258	0.031	1
40	0.392	0.073	0.168	0.335	0.031	1
45	0.308	0.088	0.155	0.420	0.030	1
50	0.219	0.107	0.138	0.509	0.026	1

Table A.4 shows the last process which is to find the surface roughness RMS value that has the smallest difference between calculation results and experimental results. In order to find an optimized roughness value, we used the ‘Solver’ function in Excel which is often used to solve the equations or find optimized values. To do this calculation, we must configure some settings in the ‘Solver’ function. We entered Excel coordinate of ‘sum of error’ at ‘set objective’ and set up to find minimum value. The Excel coordinate of surface roughness value is filled out at ‘changing variable cells’. After this setting is entered, click the ‘Solve’ button and the optimized surface roughness RMS value is obtained.

Table A.4: Surface roughness calculation using ‘Solver’ function in Microsoft Excel

Experimental Results				Calculation Results			
Input Power	1.241	→	1	1	Error (%)	Angle range consideration	Roughness RMS (μm)
Incident Angle	Output			Output			
0	0.902		0.727	0.727	0.025	0°~15°	0.135
5	0.89		0.717	0.725	-1.049	0°~20°	0.123
10	0.878		0.707	0.715	-1.029	0°~25°	0.115
15	0.844		0.680	0.692	-1.802	0°~30°	0.098
20	0.802		0.646	0.655	-1.420	0°~35°	0.085
25	0.762	→	0.614	0.604	1.571		
30	0.710		0.572	0.563	1.564		
35	0.631		0.506	0.492	3.274		
40	0.568		0.458	0.410	10.43		
45	0.471		0.379	0.321	15.43		
50	0.466		0.375	0.228	39.27		

APPENDIX B: Analysis model code in Matlab

This appendix provides the analysis model code in Matlab. The difference between in excel and in Matlab is the method used to find optimized surface roughness values. Previously, the ‘Solver’ function in excel was used. In the Matlab programming environment, we put the surface roughness value from 1nm to 1 μ m and find the quantity which satisfies the minimum difference between experimental results and calculation results. As described earlier in Chapter 3.2, the surface roughness values were always consistent with the results obtained using the Excel procedure.

```
%<TASK - 1>
%This Program get following inputs and displays surface roughness
%w:Width of Sample[mm]
%h:Height of Sample[mm]
%l:Length of Sample[mm]
%rms:Roughness(RMS) [micro meter]
%n2:Refractive index of Sample
%n1:Refractive index of Air
%Wave:Wavelength[micro meter]
%m:Mean Free Path[micro meter]
%Main:Data[Incident and Trasmission Angle, Fresnel Reflection,Roughness
Scattering]
%Cal_step1:Bulk scattering length
%Cal_step2:Bulk scattering loss at each point
%Cal_step3:Light power before roughness scattering point
%Cal_step4:Roughness scattering loss at each point
%Cal_step5:Light power before bulk scattering
%TLP:Transmitted Light Power
%Verify:Verify energy conservation in the analysis model
%=====
%preparation initialization
clear all
clc
format short g
format compact

%=====
%inputs
%=====
w=8;
l=121;
```

6 1

```
rms=0.141;
n2=1.4815;
n1=1;
Wave=0.6328;
m=509.4;
Power=1.241;

%=====
%input Chart
%=====
Input=[-5:5:75]'; %Incident Angle
Input(2,2)=0.902;
Input(3,2)=0.89;
Input(4,2)=0.878;
Input(5,2)=0.844;
Input(6,2)=0.802;
Input(7,2)=0;

for i=2:17
    Input(i,3)=Input(i,2)/Power;
end

%=====
%Calculation part for support others
%=====

Main=[-5:5:75]'; %Incident Angle

for i=2:17 %Transmission Angle
    Main(i,2)=asin(n1/n2*sin(Main(i,1)*pi/180))*180/pi;
end

for i=2:17 %Fresnel Refraction Coefficient
    Main(i,3)=(cos(Main(i,1)*pi/180)-
n2*cos(Main(i,2)*pi/180))/(cos(Main(i,1)*pi/180)+n2*cos(Main(i,2)*pi/180))^2;
end

for i=2:17 %Roughness Scattering Coefficient
    Main(i,4)=Main(i,3)*(1-exp(-
((4*pi*rms*sin(Main(i,2)*pi/180))/(Wave/n2))^2));
end

%=====
%Calclulation Part
%=====
%Step (1): Bulk scattering length
Cal_step1=[-5:5:75]';

for j=4:21 %Cal_step1 Outline
    Cal_step1(1,j)=j-4;
end

for i=2:17 %Total Scattering Length
```

```

    Cal_step1(i,3)=1/cos(Main(i,2)*pi/180);
end

for i=2:17    %Number of reflection
    Cal_step1(i,2)=fix((sin(Main(i,2)*pi/180)*Cal_step1(i,3)+w/2)/w);
end

for i=3:17    %Bulk Scattering Distance
    Cal_step1(2,4)=1;
    Cal_step1(i,5)=(w/2)/sin(Main(i,2)*pi/180);
end

for i=3:17    %Bulk Scattering Distance
    sum=0;
    for j=6:21
        sum=sum+Cal_step1(i,j-1);
        if Cal_step1(1,j)-Cal_step1(i,2)==1
            Cal_step1(i,j)=Cal_step1(i,3)-sum;
        elseif Cal_step1(1,j)-Cal_step1(i,2)<1

            Cal_step1(i,j)=w/sin(Main(i,2)*pi/180);
        else
            Cal_step1(i,j)=0;
        end
    end
end
end

%Step (2): Bulk scattering loss at each point
Cal_step2=[-5:5:75]';

%Step (3): Light power before roughness scattering point
Cal_step3=[-5:5:75]';

%Step (4): Roughness scattering loss at each point
Cal_step4=[-5:5:75]';

%Step (5): Light power before bulk scattering
Cal_step5=[-5:5:75]';

for j=4:21    %Cal_step2,3,4,5 Outline
    Cal_step2(1,j)=j-4;
    Cal_step3(1,j)=j-4;
    Cal_step4(1,j)=j-4;
    Cal_step5(1,j)=j-4;
end

for j=4:21
    Cal_step5(2,4)=1-Main(2,3);
    for i=2:17
        Cal_step5(i,5)=1-Main(i,3); %Inicial light power in the specimen
        Cal_step5(2,5)=0;
    end
end

```

```

    Cal_step2(i,j)=Cal_step5(i,j)*(1-exp(-(Cal_step1(i,j)/m))); %Bulk
    Scattering Loss

    if(Cal_step2(i,j)==0)
        Cal_step3(i,j+1)=0;
    elseif(Cal_step1(i,2)<Cal_step3(1,j))
        Cal_step3(i,j)=0;
    else
        Cal_step3(i,j)=Cal_step5(i,j)-Cal_step2(i,j); %Lightpower before
    roughness scattering point
    end

    Cal_step4(i,j)=Main(i,4)*Cal_step3(i,j); %roughness scattering loss at
    each point

    if(Cal_step4(i,j)==0)
        Cal_step5(i,j+1)=0;
    else
        Cal_step5(i,j+1)=Cal_step3(i,j)-Cal_step4(i,j); %Light power after
    roughness scattering
    end
end
end

Cal_step2(i,22)=0;
Cal_step4(i,22)=0;
for i=2:17
    for j=4:21
        Cal_step2(i,22)=Cal_step2(i,22)+Cal_step2(i,j);
        Cal_step4(i,22)=Cal_step4(i,22)+Cal_step4(i,j);
    end
end

%=====
%Calculate Transmitted Light Power
%=====
%TLP(Transmitted Light Power)
TLP=[0:5:75]';

for i=1:16

    TLP(i,2)=((cos(Main(i+1,1)*pi/180)-
n2*cos(Main(i+1,2)*pi/180))/(cos(Main(i+1,1)*pi/180)+n2*cos(Main(i+1,2)*pi/180
))^2; %Ratio of Fresnel Loss coefficient at incident surface
    TLP(i,3)=TLP(i,2)*(1-exp(-
((4*pi*rms*sin(Main(i+1,2)*pi/180))/(Wave/n2))^2)); %Roughness Scattering
Coefficient
    TLP(i,4)=1-exp(-(Cal_step1(i+1,3)/m)); %Ratio of Bulk Scattering Loss
Coefficient
    TLP(i,5)=((cos(Main(i+1,1)*pi/180)-
n2*cos(Main(i+1,2)*pi/180))/(cos(Main(i+1,1)*pi/180)+n2*cos(Main(i+1,2)*pi/180
))^2; %Ratio of Fresnel Loss coefficient at exit surface
    TLP(i,6)=(1-TLP(i,2))*(1-TLP(i,3))^(Cal_step1(i+1,2))*(1-TLP(i,4))*(1-

```

```

TLP(i,5)); % Transmitted light power
end

%=====
%Verify energy conservation in the analysis model
%=====
%TLP(Transmitted Light Power)
Verify=[0:5:75]';

for i=1:16
    Verify(i,7)=0;
    Verify(i,2)=TLP(i,6);
    Verify(i,3)=TLP(i,2);
    Verify(i,4)=Cal_step2(i+1,22);
    Verify(i,5)=Cal_step4(i+1,22);
    Verify(i,6)=TLP(i,6)*Main(i+1,3)/(1-Main(i+1,3));
    for j=2:6
        Verify(i,7)=Verify(i,7)+Verify(i,j);
    end
end

%=====
%calculating transmitted light power using various roughness values
%=====

for i=2:17 %Ratio of Bulk Scattering Loss at each point
    for j=4:21
        Main(i,j+2)=exp(-(Cal_step1(i,j)/m));
    end
end

for i=2:17 %Number of reflection
    Main(i,5)=fix((sin(Main(i,2)*pi/180)*Cal_step1(i,3)+w/2)/w);
end

Results=[-5:5:75]';
a=0.001;
for i=2:1001

    Results(1,i)=a;
    a=a+0.001;
end

mult=0;
for c=2:1001
    for i=2:17
        Main(i,4)=Main(i,3)*(1-exp(-
((4*pi*Results(1,c)*sin(Main(i,2)*pi/180))/(Wave/n2))^2)); %Roughness
        Scattering Coefficient
        mult=(1-Main(i,3))^2*(1-Main(i,4))^(Cal_step1(i,2));
        for j=6:23
            mult=mult*Main(i,j);
        end
    end
end

```

6 5

```
        end
        Results(i,c)=mult;
        mult=0;
    end
end

%=====
%Solver until 20 Degree
%=====
for j=2:1001
    Input(1,j+2)=Results(1,j);
    sum=0;
    for i=2:6
        sum=sum+(Input(i,3)-Results(i,j))^2;
    end
    Input2(1,j-1)=sum;
end

[i,j]=find(Input2==min(min(Input2))); [i,j];
j=j/1000;
disp(['Optimized RMS (0~20 Degree) = ',num2str(j) ' micrometer'])

%=====
%Solver until 15 Degree
%=====
for j=2:1001
    Input(1,j+2)=Results(1,j);
    sum=0;
    for i=2:5
        sum=sum+(Input(i,3)-Results(i,j))^2;
    end
    Input3(1,j-1)=sum;
end

[i,j]=find(Input3==min(min(Input3))); [i,j];
j=j/1000;
disp(['Optimized RMS (0~15 Degree) = ',num2str(j) ' micrometer'])

%=====
%Solver until 10 Degree
%=====
for j=2:1001
    Input(1,j+2)=Results(1,j);
    sum=0;
    for i=2:4
        sum=sum+(Input(i,3)-Results(i,j))^2;
    end
    Input4(1,j-1)=sum;
end

[i,j]=find(Input4==min(min(Input4))); [i,j];
j=j/1000;
disp(['Optimized RMS (0~10 Degree) = ',num2str(j) ' micrometer'])
```